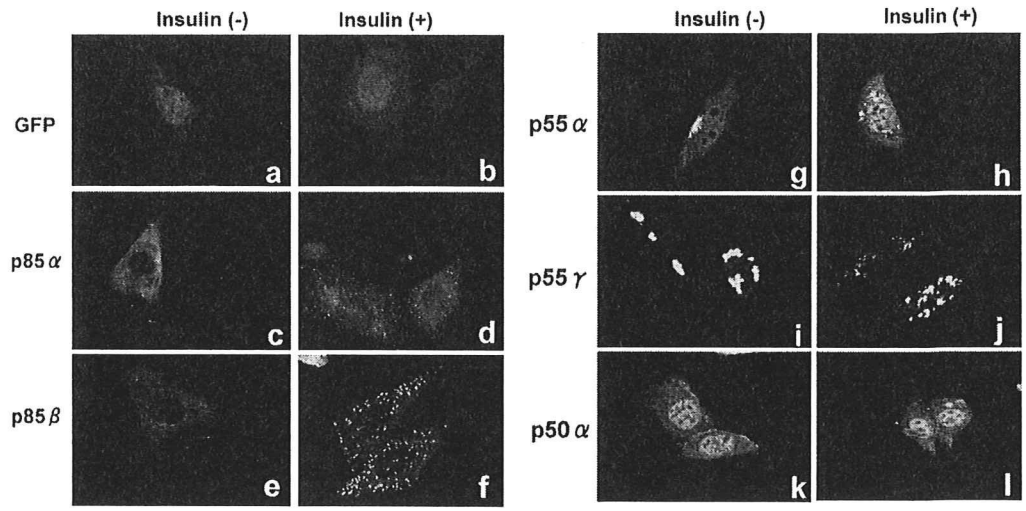

Fig. 1. The localizations of each PI 3-kinase regulatory subunit-GFP protein in CHO-IR cells in the absence and presence of insulin. CHO-IR cells were seeded onto a 60-mm plastic culture dish at 6×10^5 cells/dish. The following day, transfection procedures were performed using 30 μl of lipofectamine diluted in 300 μl of Opti-MEM I and 6 μg of pSRα vector DNA containing cDNA of GFP (a,b), p85α-GFP (c,d), p85β-GFP (e,f), p55α-GFP (g,h), p55γ-GFP (i,j), and p50α-GFP (k,l). Cells were incubated in the presence of the lipofectamine-DNA mix for 5 h, and then incubated overnight in DMEM containing 10% FCS. Forty-eight hours after transfection, each of the transfected 60-mm dishes was used for experiments. Before the experiments, CHO-IR cells were serum starved and stimulated with insulin for 10 min (b, d, f, h, j, and l). The results shown are representative of three experiments.

pressed (data not shown). Interestingly, only the signals observed in an immunofluorescence study using antibodies against IRS-1 corresponded to with these foci (Fig. 2h), suggesting that IRS-1 co-localized with these p85 foci in response to insulin. Though we cannot rule out the possibility that the p85-IRS-1 complex contains other unex-

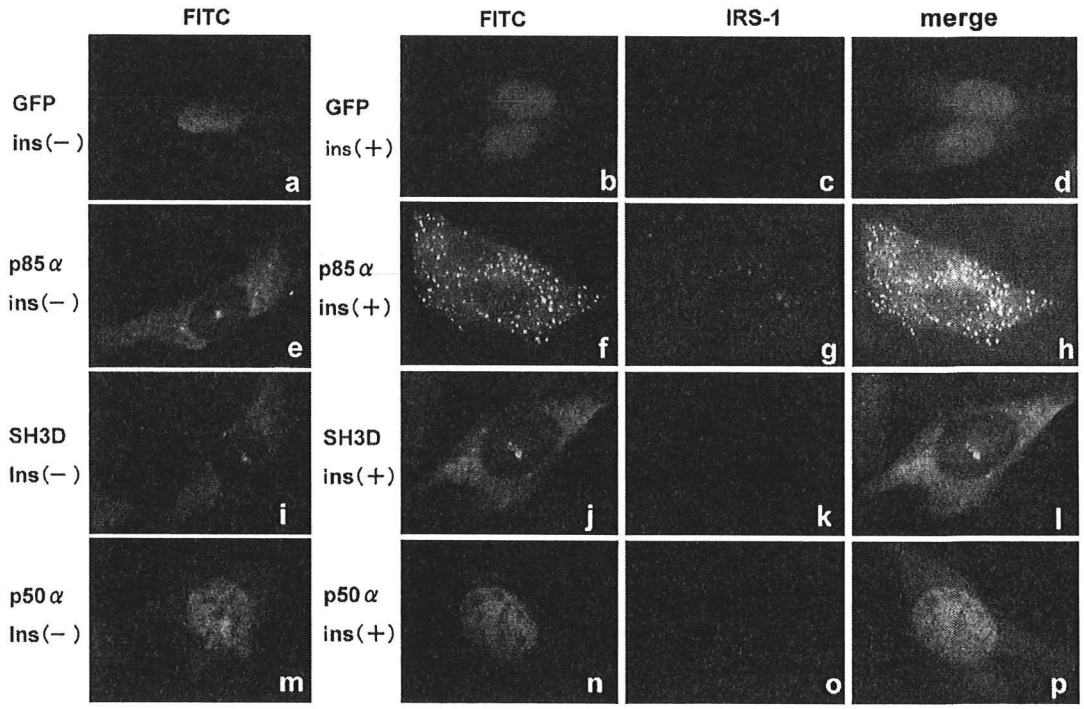

Fig. 2. Immunofluorescence analyses of PI 3-kinase regulatory subunit-GFP proteins. CHO-IR cells were plated at near-confluent density and were transfected with GFP (a–d), p85α-GFP (e–h), SH3D-GFP (i–l) or p50α-GFP(m–p). Cells were serum starved and stimulated with insulin for 10 min. Cells were fixed in 4% paraformaldehyde–PBS for 20 min, then quenched for 15 min in 0.2% Triton X-100. Commercial primary antibodies against IRS-1 were diluted in 0.1% horse serum–PBS, and incubations were carried out at 4 °C overnight. TRITC-conjugated anti-mouse immunoglobulin secondary antibody diluted in 0.1% horse serum-PBS was applied after three 5 min washes in PBS. After a 1 h incubation, coverslips were mounted in 1% propyl gallate–50% glycerol–PBS and were observed under a microscope. Results shown are representative of three experiments.

pected proteins, both the insulin receptor and p110α catalytic subunits are absent from these foci according to immunofluorescence results, suggesting that only p85 and the IRS-1 dimer form a sequestration complex in response to insulin. As p55s and p50α did not form foci, we expected that the domain responsible for IRS-1 complex formation would be either the SH3 domain or the bcr homology (BH) domain. Thus, we prepared and overexpressed the SH3 domain deletion mutant (SH3D) of p85α-GFP in CHO-IR cells. This mutant failed to form foci (Fig. 2j), i.e., the SH3 domain of regulatory subunits is likely to be responsible for formation of the p85-IRS-1 sequestration complex. Based on a previous report that SH3 domain-proline rich motif inertactions mediate dimerization of PI-3 kinase regulatory subunits [18], we examined whether these interactions are involved in formation of the sequestration complex with IRS-1. After confirming that β-galactosidase, as a positive control peptide, was properly transfected in our experiments (Supplementary Fig. 2a), proline-rich motif peptides were similarly transfected into CHO-IR cells. As shown in Supplementary Fig. 2e, proline-rich peptides did not affect p85-IRS-1 complex formation, indicating that SH3-domain-proline-rich motif interactions are unlikely to be involved in this complex formation.

Though p85α-IRS-1 complexes formed in response to insulin stimulation, as demonstrated by immunofluorescence analysis, we attempted to further demonstrate these direct associations by immmunoprecipitation. After confirming that almost equal amounts of p85α, SH3D, and p50α-GHP proteins had been expressed in CHO-IR cells (Fig. 3, upper panel), we performed immunoprecipitation experiments using either anti-IRS-1 or anti-GFP antibody and blotted the transferred sheets with anti-GFP or anti-phopho-tyrosine antibody (4G10), respectively. As expected, an insulin-dependent IRS-1 association with p85α-GFP was detected (Fig. 3, middle and lower panels). Despite the lack of IRS-1 complex formation, IRS-1 associations with both the SH3D mutant and p50α-GFP were also observed. Moreover, only IRS-1-SH3D mutant binding was present in the absence of insulin stimulation. Thus, even though the overexpressed regulatory subunits fail to form discrete foci, these subunits do actually bind to IRS-1 in the presence of insulin.

Next, we investigated downward signaling by analyzing Ser473-Akt phosphorylation in the presence of insulin with overexpression of each isoform. As shown in Fig. 4, p85α and SH3D mutant-GFP overexpressions markedly diminished insulin dependent Akt phosphorylations, while p50α-GFP overexpression did not affect Akt phosphorylation as compared with control cells. Based on a previous report demonstrating monomeric p85 to down-regulate insulin signaling by competing with the p85-p110 dimer for IRS-1 binding [12], p85α-GFP and the SH3D mutant also negatively suppressed insulin signaling by removing IRS-1 from p85-p110-IRS trimers.

Discussion

In this study, we overexpressed five class IA PI 3-kinase regulatory subunit isoforms tagged with GFP in CHO-IR cells and investigated intracellular localizations in response to insulin stimulation. p85α and p85β redistributed to discrete foci in CHO-IR cells, while other isoforms did not. p55α and p55γ preferentially remained in the perinuclear

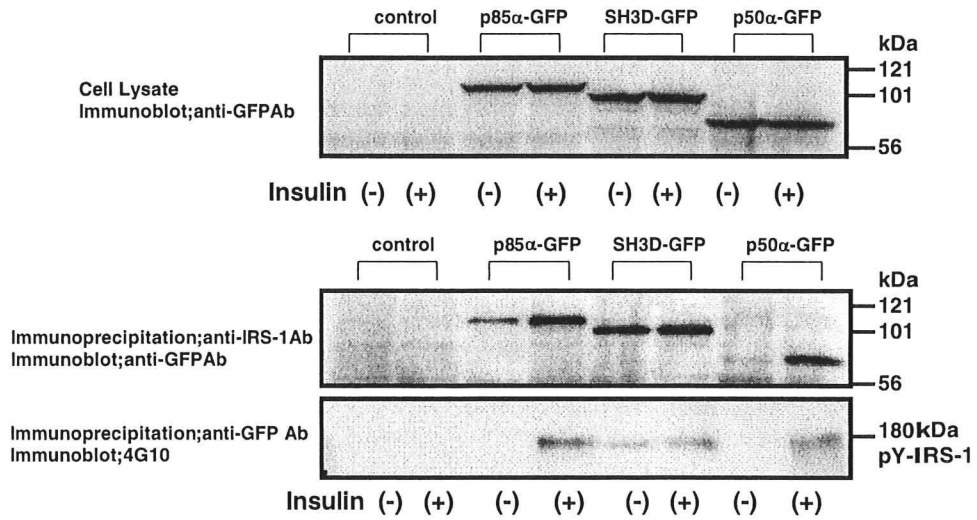

Fig. 3. Direct associations between IRS-1 proteins and each PI 3-kinase regulatory subunit isoform. CHO-IR cells were transfected with only the pSRα vector, pSRα DNA containing cDNA of p85α-GFP, SH3D-GFP, or p50α-GFP. After serum starvation, cells were stimulated with insulin for 10 min. Supernatants including tissue protein extracts were resolved on 10% SDS–polyacrylamide gel, followed by electrophoretic transfer to a nitrocellulose membrane. Membranes were incubated for 1 h at RT with anti-GFP antibody. After blotting with anti-GFP antibody, detection was performed using an ECL chemiluminescence kit (upper panel). Immunoprecipitation was performed using anti-IRS-1 (middle panel) and GFP antibodies (lower panel). Immunoprecipitates were then boiled in Laemmli sample buffer, subjected to SDS–PAGE, and finally to Western blotting using anti-GFP (middle panel) and anti-phosphotyrosine antibodies (lower panel). Three independent experiments were performed and similar results were obtained.

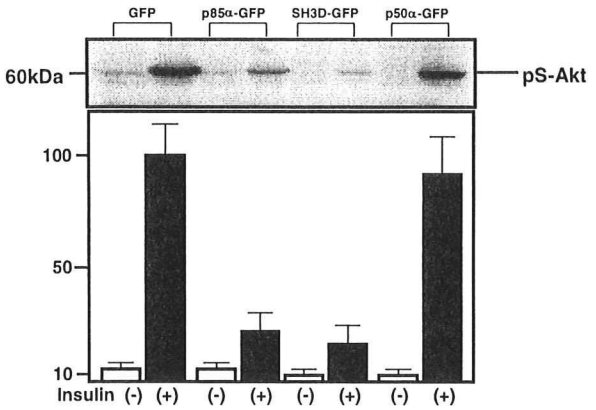

Fig. 4. Effects of overexpressing each isoform of the PI 3-kinase regulatory subunit on Ser473-Akt phosphorylation in CHO-IR cells. CHO-IR cells were transfected with only pSRα vector, pSRα DNA containing cDNA of p85α-GFP, SH3D-GFP or p50α-GFP. After serum starvation, cells were stimulated with insulin for 10 min. Supernatants including tissue protein extracts were resolved on 10% SDS–polyacrylamide gel, followed by electrophoretic transfer to a nitrocellulose membrane. Membranes were incubated for 1 h at RT with anti-phospho-Akt (Ser473) antibody. After blotting with the indicated secondary antibody, detection was performed using an ECL chemiluminescent kit. Quantitations were performed using a Molecular Imager. Three independent experiments were performed and similar results were obtained.

region, while p50α exhibited localizations very similar to that of the control GFP. The signal sequence of p55s is located in the N-terminal domain, which is composed of a unique 34 amino-acid sequence. It was previously reported that this 34 amino-acid sequence has a high affinity for α/β tubulin [19] or the retinoblastoma tumor suppressor protein (Rb), a key regulator of cell cycle progression [20]. Further study is needed to investigate whether perinuclear localizations are related to the associations with these proteins.

Though PI 3-kinase plays a key role in mediating insulin signals downstream from IRS-1, mice lacking the p85α or p85β subunits of PI 3-kinase, paradoxically, show high insulin sensitivity [21,22]. There are two possible explanations for this discrepancy. First, p50α subunits were previously demonstrated to exhibit a markedly higher capacity for activation of associated PI 3-kinase via insulin stimulation and to have a higher affinity for tyrosine-phosphorylated IRS-1 than other isoforms [10]. In mice lacking p85s, there are more p50α subunits and they substitute for the missing p85s subunits [21,22], thereby producing enhanced insulin sensitivity. In fact, the overexpression of p50α-GFP also resulted in high insulin sensitivity being maintained in this study. Second, p85s regulatory subunits have two SH2 domains separated by an inter-SH2 domain, through which they bind p110 catalytic subunits, and in addition, monomeric p85s and p85s–p110s mutually compete for IRS-1 binding [12]. Thus, the molecular balance between p85s and p110s might have a major effect on insulin signaling downstream from PI 3-kinase. We can speculate that fewer p85s subunits means greater insulin sensitivity. Inversely, if an excess of monomeric p85s is present, insulin signaling might be inhibited by p85s-IRS-1 dimers, which have no ability to transmit insulin signals, and thus serve as a dominant negative form.

Subsequently, it was clearly demonstrated that p85α-IRS-1 dimers form a sequestration complex in response to IGF-1 stimulation [11]. We observed similar p85-IRS-1 complexes in the case of insulin stimulation in p85s-GFP transfected CHO-IR cells and showed the p85α-SH3 domain to be responsible for complex formation. Based on a previous report describing the isolated p85α-SH3 domain as binding only one of its endogenous proline-rich motifs, PRM1 (Fig. 1) [18], we examined whether SH3-PRM1 interactions are involved in forming the sequestration complex with IRS-1. However, PRM1 peptides were incapable of disrupting the p85α-IRS-1 complex, suggesting that other interactions with the SH3 domain, such as the SH3-BH domain [23], might be involved in this complex formation.

In conclusion, when five PI 3-kinase regulatory subunit isoforms tagged in their C-terminal tails with GFP were overexpressed in CHO-IR cells, only p85α and p85β redistributed to discrete foci in response to insulin. We immunohistochemically demonstrated that these isolated foci are composed of p85 and IRS-1 and found the SH3 domain located in the N-terminal portion of p85 to be responsible for the formation of foci with IRS-1. These p85-IRS-1 complex formations represent negative regulation of insulin signaling due to a molecular imbalance between p85s and p110s.

Appendix A. Supplementary data

Supplementary data associated with this article can be found, in the online version, at doi:10.1016/j.bbrc.2007.10.187.

References

[1] B. Cheatham, C.J. Vlahos, L. Cheatham, L. Wang, J. Blenis, C.R. Kahn, Phosphatidylinositol 3-kinase is required for insulin stimulation of pp70 S6 kinase, DNA synthesis, and glucose transporter translocation, Mol. Cell. Biol. 14 (1994) 4902–4911.

[2] K. Kimura, S. Hattori, Y. Kabuyama, Y. Shizawa, J. Takayanagi, S. Nakamura, S. Toki, Y. Matsuda, K. Onodera, Y. Fukui, Neurite outgrowth of PC12 cells is suppressed by wortmannin, a specific inhibitor of phosphatidylinositol 3-kinase, J. Biol. Chem. 269 (1994) 18961–18967.

[3] S. Wennstrom, P. Hawkins, F. Cooke, K. Hara, K. Yonezawa, M. Kasuga, T. Jackson, L. Claesson-Welsh, L. Stephens, Activation of phosphoinositide 3-kinase is required for PDGF-stimulated membrane ruffling, Curr. Biol. 4 (1994) 385–393.

[4] R. Yao, G.M. Cooper, Requirement for phosphatidylinositol-3 kinase in the prevention of apoptosis by nerve growth factor, Science 267 (1995) 2003–2006.

[5] H. Katagiri, T. Asano, H. Ishihara, K. Inukai, Y. Shibasaki, M. Kikuchi, Y. Yazaki, Y. Oka, Overexpression of catalytic subunit p110alpha of phosphatidylinositol 3-kinase increases glucose transport activity with translocation of glucose transporters in 3T3-L1 adipocytes, J. Biol. Chem. 271 (1996) 16987–16990.

[6] D.J.V. Horn, M.G. Myers Jr., J.M. Backer, Direct activation of the phosphatidylinositol 3′-kinase by the insulin receptor, J. Biol. Chem. 269 (1994) 29–32.
[7] P. Hu, A. Mondino, E.Y. Skolnik, J. Schlessinger, Cloning of a novel, ubiquitously expressed human phosphatidylinositol 3-kinase and identification of its binding site on p85, Mol. Cell. Biol. 13 (1993) 7677–7688.
[8] S. Pons, T. Asano, E. Glasheen, M. Miralpeix, Y. Zhang, T.L. Fisher, M.G. Myers, X.J. Sun, M.F. White, The structure and function of p55PIK reveal a new regulatory subunit for phosphatidylinositol 3-kinase, Mol. Cell. Biol. 15 (1995) 4454–4465.
[9] K. Inukai, M. Anai, E.V. Breda, T. Hosaka, H. Katagiri, M. Funaki, Y. Fukushima, T. Ogihara, Y. Yazaki, M. Kikuchi, Y. Oka, T. Asano, A novel 55-kDa regulatory subunit for phosphatidylinositol 3-kinase structurally similar to p55PIK Is generated by alternative splicing of the p85α gene, J. Biol. Chem. 271 (1996) 5317–5320.
[10] K. Inukai, M. Funaki, T. Ogihara, H. Katagiri, A. Kanda, M. Anai, Y. Fukushima, T. Hosaka, M. Suzuki, B.S. Shin, K. Takata, Y. Yazaki, M. Kikuchi, Y. Oka, T. Asano, p85α gene generates three isoforms of regulatory subunit for phosphatidylinositol 3-kinase (PI 3-Kinase), p50α, p55α, and p85α, with different PI 3-kinase activity elevating responses to insulin, J. Biol. Chem. 272 (1997) 7873–7882.
[11] J. Luo, S.J. Field, J.Y. Lee, J.A. Engelman, L.C. Cantley, The p85 regulatory subunit of phosphoinositide 3-kinase down-regulates IRS-1 signaling via the formation of a sequestration complex, J. Cell Biol. 170 (2005) 455–464.
[12] K. Ueki, P. Algenstaedt, F. Mauvais-Jarvis, C.R. Kahn, Positive and negative regulation of phosphoinositide 3-kinase dependent signaling pathways by three different gene products of the p85 α regulatory subunit, Mol. Cell. Biol. 20 (2000) 8035–8046.
[13] K. Inukai, M. Funaki, M. Anai, T. Ogihara, H. Katagiri, Y. Fukushima, H. Sakoda, Y. Onishi, H. Ono, M. Fujishiro, M. Abe, Y. Oka, M. Kikuchi, T. Asano, Five isoforms of the phosphatidylinositol 3-kinase regulatory subunit exhibit different associations with receptor tyrosine kinase and their tyrosine phosphorylations, FEBS Lett. 490 (2001) 32–38.
[14] K. Inukai, A.M. Shewan, W.S. Pascow, S. Katayama, D.E. James, Y. Oka, Carboxy terminus of glucose transporter 3 contains an apical targeting domain, Mol. Endocrinol. 18 (2004) 339–349.
[15] K. Inukai, M. Watanabe, Y. Nakashima, N. Takata, A. Isoyama, T. Sawa, S. Kurihara, T. Awata, S. Katayama, Glimepiride enhances intrinsic peroxisome proliferator-activated receptor-gamma activity in 3T3-L1 adipocytes, Biochem. Biophys. Res. Commun. 328 (2005) 484–490.
[16] K. Imai, K. Inukai, Y. Ikegami, T. Awata, S. Katayama, LKB1, an upstream AMPK kinase, regulates glucose and lipid metabolism in cultured liver and muscle cells, Biochem. Biophys. Res. Commun. 351 (2006) 595–601.
[17] M. Funaki, H. Katagiri, A. Kanda, M. Anai, M. Nawano, T. Ogihara, K. Inukai, Y. Fukushima, H. Ono, Y. Yazaki, M. Kikuchi, Y. Oka, T. Asano, p85/p110-type phosphatidylinositol kinase phosphorylates not only the D-3, but also the D-4 position of the inositol ring, J. Biol. Chem. 274 (1999) 22019–22024.
[18] A.G. Harpur, M.J. Layton, P. Das, M.J. Bottomley, G. Panayotou, P.C. Driscoll, M.D. Waterfield, Intermolecular interactions of p85α regulatory subunit of phosphoatidylinositol 3-kinase, J. Biol. Chem. 274 (1999) 12323–12332.
[19] K. Inukai, M. Funaki, M. Nawano, H. Katagiri, T. Ogihara, M. Anai, Y. Onishi, H. Sakoda, H. Ono, Y. Fukushima, M. Kikuchi, Y. Oka, T. Asano, The N-terminal 34 residues of the 55 kDa regulatory subunits of phosphoinositide 3-kinase interact with tubulin, Biochem. J. 346 (2000) 483–489.
[20] X. Xia, A. Cheng, D. Akinmade, A.W. Hamburger, The N-terminal 24 amino acids of the p55g regulatory subunit of phosphoinositide 3-kinase binds Rb and induce cell cycle arrest, Mol. Cell. Biol. 23 (2003) 1717–1725.
[21] Y. Terauchi, Y. Tsuji, S. Satoh, H. Minoura, K. Murakami, A. Okuno, K. Inukai, T. Asano, Y. Kaburagi, K. Ueki, H. Nakajima, T. Hanafusa, Y. Matsuzawa, H. Sekihara, Y. Yin, J.C. Barrett, H. Oda, T. Ishikawa, Y. Akanuma, I. Komuro, M. Suzuki, K. Yamamura, T. Kodama, H. Suzuki, T. Kadowaki, Increased insulin sensitivity and hypoglycemia in mice lacking the p85α subunit of phosphatidylinositide 3-kinase, Nat. Genet. 21 (1999) 230–235.
[22] K. Ueki, C.M. Yballe, S.M. Brachmann, D. Vicent, J.M. Watt, C.R. Kahn, L.C. Cantley, Increased insulin sensitivity in mice lacking p85β subunit of phosphoinositide 3-kinase, Proc. Natl. Acad. Sci. USA 99 (2002) 419–424.
[23] A. Musacchio, L.C. Cantley, S.C. Harrison, Crystal structure of the breakpoint cluster region-homology domain from phosphoinositide 3-kinase p85 α subunit, Proc. Natl. Acad. Sci. USA 93 (1996) 14373–14378.

DIABETES RESEARCH AND CLINICAL PRACTICE 79 (2008) 2–10

available at www.sciencedirect.com

ScienceDirect

journal homepage: www.elsevier.com/locate/diabres

Regulation of gut-derived resistin-like molecule β expression by nutrients

Junko Fujio [a,b], *Akifumi Kushiyama* [b], *Hideyuki Sakoda* [b], *Midori Fujishiro* [b], *Takehide Ogihara* [c], *Yasushi Fukushima* [a], *Motonobu Anai* [d], *Nanao Horike* [a], *Hideaki Kamata* [e], *Yasunobu Uchijima* [a], *Hiroki Kurihara* [a], *Tomoichiro Asano* [a,e,*]

[a] *Department of Physiological Chemistry and Metabolism, Graduate School of Medicine, University of Tokyo, 7-3-1 Hongo, Bunkyo-ku, Tokyo 113-0033, Japan*

[b] *Department of Internal Medicine, Graduate School of Medicine, University of Tokyo, 7-3-1 Hongo, Bunkyo-ku, Tokyo 113-0033, Japan*

[c] *Division of Advanced Therapeutics for Metabolic Diseases, Center for Translational and Advanced Animal Research on Human Diseases, Tohoku University Graduate School of Medicine, 2-1 Seiryo-machi, Sendai, Japan*

[d] *Institute for Adult Diseases, Asahi Life Foundation, 1-6-1 Marunouchi, Chiyoda-ku, Tokyo 100-0005, Japan*

[e] *Department of Medical Science, Graduate School of Medicine, University of Hiroshima, 1-2-3 Kasumi, Minami-ku, Hiroshima City, Hiroshima 734-8551, Japan*

ARTICLE INFO

Article history:
Received 25 August 2006
Received in revised form
19 February 2007
Accepted 16 April 2007
Published on line 23 October 2007

Keywords:
RELMβ
Nutrient compositions
Insulin resistance

ABSTRACT

Resistin was initially identified as a protein, secreted by adipocytes, which inhibits insulin action and adipose differentiation. The three proteins homologous to resistin were identified and given the names resistin-like molecules (RELM) α, β and γ. Resistin and RELMα are abundantly expressed in adipose, but RELMβ and RELMγ are secreted mainly from the gut. Since nutrient composition greatly affects insulin sensitivity, we investigated the regulatory effects of various nutritional factors in food on the expressions of resistin family proteins.

First, mice were given diets with different nutritional compositions (high-carbohydrate, high-protein and high-fat) for 2 weeks. RELMβ mRNA expression in the intestines was markedly suppressed by the high-protein and high-carbohydrate diets, while slightly but not significantly upregulated by the high-fat diet. In the epididymal fat, resistin expression was unchanged, while RELMα expression was markedly decreased by the high-carbohydrate diet. Taking into consideration that humans have neither RELMα nor RELMγ, our subsequent studies focused on RELMβ expression. We used the human colon cancer cell line LS174T. Treatments with insulin and TNFα as well as stearic acid, a saturated free fatty acid, upregulated RELMβ expression, while D-glucose downregulated RELMβ. These results suggest RELMβ expression to be regulated directly by nutrients such as glucose and saturated free fatty acids including stearic acid, as well as by hormones including insulin and TNFα. These regulations may play an important role in the nutrient-associated induction of insulin resistance.

* *Corresponding author.* Tel.: +81 82 257 5135; fax: +81 82 257 5136.
E-mail address: asano-tky@umin.ac.jp (T. Asano).

0168-8227/$ – see front matter © 2007 Elsevier Ireland Ltd. All rights reserved.
doi:10.1016/j.diabres.2007.04.015

1. Introduction

Resistin and its related proteins, *i.e.* resistin-like molecules (RELMs) α, β and γ, are a family of recently identified proteins [1,2]. They share an N-terminal signal sequence and a C-terminal region with a unique structure that contains 10 cysteine residues [3]. Resistin was identified as an adipocyte secreted factor, expression of which is increased in genetically obese (*ob/ob* and *db/db*) mice [4]. Furthermore, administration of resistin reportedly impairs glucose tolerance and reduces insulin action in normal mice, both of which are reversed by immunoneutralization with anti-resistin antibody [4]. Resistin knock-out mice were also described as having lower fasting blood glucose [5]. However, there are conflicting observations regarding its function as a factor responsible for insulin resistance [6–9].

RELMα is a secreted protein of 111 amino acids that has been identified in rats and mice and is expressed in the lungs, white adipose tissue and the intestines. There is a difference between the two species in that RELMα expression in white adipose tissue is much lower in rats than in mice [2,3]. This protein has been shown to inhibit the differentiation of adipocytes *in vitro* [10]. RELMα is induced by Th2 type cytokines in rodent pulmonary epithelial cells, and thus is likely to be involved in the inflammatory response [11]. RELMγ was also initially identified in the nasal respiratory epithelium of rats [2], and was revealed to be expressed in bone marrow, peripheral blood granulocytes, the spleen, lungs and pancreas as well as the large and small intestines of mice [2,12,13].

RELMβ is highly expressed in goblet cells of the murine colon and secreted in response to bacterial colonization [14], and thus was suggested to play an important role in defense against nematode parasitization in mice [15]. On the other hand, we previously reported that RELMβ and RELMγ are present in blood, and that their serum concentrations and expressions in the colon were elevated in insulin resistant models such as obese *db/db* mice and high-fat-fed mice [16]. In addition, transgenic mice which overexpressed RELMβ in the liver, exhibited hyperglycemia, hyperlipidemia and fatty liver [17]. Thus, we consider intestine-derived RELMβ to be involved in insulin resistance.

The first objective of this study was to investigate the regulatory effects of nutritional factors in different diets on the expressions of resistin and RELMs. Interestingly, the expression of RELMβ, but not resistin, was found to be strongly influenced by different dietary compositions. Although there are four genes encoding this protein family in the mouse, only resistin and RELMβ have been identified in the human genome sequence [2]. Thus, we focused on the regulation of RELMβ expression, and performed additional experiments using cultured cells to examine whether nutritional factors, as well as hormones such as insulin and TNFα, are direct regulators of RELMβ expression. Herein, we show the regulation of gut-derived RELMβ to be regulated by both nutrients and hormones, and that its upregulation may be involved in the pathogenesis of diet-derived insulin resistance.

2. Materials and methods

2.1. Reagents and antibodies

All reagents were of analytical grade and anti-RELMβ antibody was purified as previously described [17].

2.2. Animal studies

Six-week-old mice (C57BL/6J) were purchased from CLEA Inc and housed under conventional conditions. All animal studies were performed after 2–3 days acclimation period and mice were anesthetized with pentobarbital. To determine RELMβ expression levels in fed and fasted states, the colon was excised from both mice fed *ad libitum* and those fasted for 18 h ($n = 3$ per group). In the fasted state, both the colon and the ileum were collected to assess the correlation between RELMβ mRNA levels in these tissues ($n = 22$). In the dietary studies, animals were divided into four groups receiving different diets, *i.e.* high-carbohydrate (CA), high-protein (P), high-fat (HF) and control (C) diets, and were fed *ad libitum* for 2 weeks ($n = 4$–5 per group) or fed once ($n = 6$ per group), to assess both acute and chronic effects of these diets. The compositions of the diets are shown in Table 1. With 2 week feeding, at the end of the 2-week period, the animals were fasted for 18 h. Then, blood, colon and epididymal fat, as a representative white adipose tissue, samples were collected. Tissue samples were homogenized in an adequate amount of ice-cold Isogen (Nippon Gene) directly for mRNA extraction or ice-cold Lysis Buffer (10 mM HEPES pH 7.4, 150 mM NaCl, 2 mM EDTA, 1% Triton-X 100, 2 mM PMSF, 2 μg/ml aprotinin, 5 μg/ml leupeptin) after careful removal of stool, for Western blotting. Serum was separated, after a sufficient time at room temperature to allow coagulation, by centrifugation at 3000 rpm for 20 min followed by 1 min at 15000 rpm. Lipid and other parameters were measured in the sera obtained.

Animal care and procedures for the experiments were performed according to the Japanese guidelines for the care and use of experimental animals.

Table 1 – Dietary compositions

	Control diet (3.58 Kcal/g)		High carbohydrate (3.55 kcal/g)		High protein diet (3.47 kcal/g)		High fat diet (6.66 kcal/g)	
	%weight	%kcal	%weight	%kcal	%weight	%kcal	%weight	%kcal
Protein	23.3	26	13	14	70	79.8	24.2	14.6
Fat	5.3	13.3	1	4.4	1	5.7	60	81
Carbohydrate	53.8	60.1	80	81.6	10	12.5	7.3	4.4

2.3. *Intraperitoneal glucose tolerance tests*

Glucose tolerance tests were performed after the 2-week feeding period. After an overnight fast, 2 g/kg D-glucose was injected intraperitoneally after the initial glucose measurement. Glucose levels were again determined at 15, 30, 60, 90 and 120 min after the injection. Glucose was measured by tail snipping. Three or four mice from each group were subjected to this test.

2.4. *Cell culture*

LS174T cells were obtained from the Cell Resource Center for Biomedical Research (Sendai, Japan), and cultured in RPMI 1640 (Sigma) medium supplemented with 10% FCS (Invitrogen), Penicillin 100 U/ml and Streptomycin 100 μg/ml (GIBCO Invitrogen) at 37 °C in 5% CO_2. Cells were cultured on 24 well plates (IWAKI) for the extraction of mRNA for stimulation tests. At 80% confluence, each well was washed twice with PBS and subsequently incubated under various conditions described below for 24 h, and the cells were then subjected to the mRNA extraction.

For insulin and TNFα stimulation, insulin and TNFα were added to RPMI 1640 to give final concentrations of 100 nM and 100 ng/ml, respectively. For glucose stimulation, RPMI 1640 supplemented with D-glucose to achieve final concentrations of 5, 11 or 25 mM was used and RPMI 1640 containing L-glucose at the same concentrations was used for the controls. Furthermore, linoleic acid (LA), oleic acid (OA) and stearic acid (SA) resolved in ethanol and conjugated with 20% bovine serum albumin (BSA) were added to RPMI 1640 to give two final concentrations, 0.5 and 2.0 mM, for each FFA. For control samples, medium adjusted only with ethanol and BSA was used.

2.5. *RNA isolation and quantification by real time quantitative polymerase chain reaction*

Total RNA was extracted from murine tissue samples, or cultured LS174T cells, using Isogen (Nippon Gene) according to the manufacturer's instructions. The cDNA was synthesized from total RNA using a First Strand cDNA Synthesis Kit for RT-PCR (Roche Diagnostics) according to the manufacturer's instructions. The oligonucleotide primers were designed using program Primer 3 (http://frodo.wi.mit.edu/cgi-bin/primer3/) and produced by Japan Bio Service, (Saitama, Japan). mRNA expressions for RELMs and resistin were quantified on a Light Cycler Instrument (Roche) using Light Cycler DNA Master SYBR Green I. The results were standardized against internal controls, m36B4 or h36B4 for the mouse tissue and LS174T cell-derived mRNA, respectively. The primer sequences used for human RELMβ (hRELMβ), mouse resistin (mResistin), mouse RELMβ (mRELMβ), mouse RELMγ (mRELMγ), m36B4 and h36B4 are shown in Table 2. The primers for hRELMβ and h36B4 were used as described previously [14,18].

2.6. *Histological analysis*

Colonic tissues were routinely embedded in paraffin; approximately 5 μm-thick slices were obtained from these samples. Slices were stained with hematoxylin and eosin (HE) to compare the number of goblet cells. Immunostaining was performed according to the microwave antigen-retrieval technique, using purified anti-mRELMβ antibody (1:500) and a VECSTATIN ABC kit (Vector labs), following the manufacturer's instructions.

2.7. *Western blotting*

Twenty micrograms of protein extracted from homogenized colonic tissue or 4 μl of serum was boiled in Laemmli sample buffer containing 100 mmol/l dithiothreitol. Samples were subjected to SDS-PAGE, transferred to Hybond-P membranes (GE Healthcare, Bioscience Inc.), and immunoblotted using purified anti-mRELMβ antibody (1:1000). Proteins were visualized with enhanced chemiluminescence (ECL) and exposed to ECL film (GE Healthcare, Bioscience Inc.). The band intensity was analyzed as described previously [16].

2.8. *Statistical analysis*

Stat View-J 5.0 software for windows (SAS Institute Inc.) was used for statistical analysis. Results are expressed as mean ± S.E. In the multiple comparisons, ANOVA followed by the post hoc Fisher's PLSD test was used to compare means between pairs of groups. The unpaired *t*-test was also used to compare means between pairs of groups.

3. Results

3.1. *Characterizations of feeding groups, energy intake and changes in serum lipid, glucose and insulin levels*

The body weights, epididymal fat weights, glucose levels, insulin levels and serum lipid levels at the start and after 2

Table 2 – Primers used for real-time PCR

	Sense	Antisense
m-Resistin	TCATTTCGCCTCCTTTTCCT	AAGCGACCTGCAGCTTACA
m-RELMα	TCCAGCTAACTATCCCTCCACTGT	CAGTAGCAGTCATCCCAGCA
m-RELMβ	CAAAAAGCTAGAACTGAGCTCCAG	TAGTAATATGAAGACAATGAGTCAGG
m-RELMγ	CTTGCCAATCGAGATGACTG	TTTCCAAGTTGGGATTGTGC
m-36B4	GCTCCAAGCAGATGCAGCA	CCGGATGTGAGGCAGCAG
h RELMβ	CACCCAGGAGCTCAGAGATCTAA	ACGGCCCCATCCTGTACA
h-36B4	CCACGCTGCTGAACATGCT	TCGAACACCTGCTGGATGAC

Table 3a – Characteristics of the dietary groups of the study

	Control	High carbohydrate	High protein	High fat
Body weight (g)	19.2 ± 0.32	19.2 ± 0.15	19.4 ± 0.33	19.2 ± 0.22
Blood glucose (mg/dl)	66.4 ± 3.24	67.8 ± 6.34	64.7 ± 4.21	57.9 ± 3.03
Insulin (ng/ml)	2.91 ± 0.09	3.20 ± 0.31	2.80 ± 0.50	3.72 ± 0.17
Triglyceride (mg/dl)	73.8 ± 5.32	69.6 ± 4.47	76.3 ± 6.56	65.9 ± 3.40
Cholesterol (mg/dl)	82.6 ± 3.07	61.8 ± 6.51	84.6 ± 4.79	80.5 ± 7.27
NEFA (μEq/l)	1.33 ± 0.06	1.28 ± 0.18	1.14 ± 0.07	1.00 ± 0.05

Values are indicated as mean ± S.E. (n = 4–6).
No statistically significant differences between the feeding groups were observed.

Table 3b – Characteristics of the dietary groups at the end of the 2-week feeding period

	Control	High carbohydrate	High protein	High fat
Body weight (g)	21.1 ± 0.6	20.4 ± 0.6	19.7 ± 1.0	23.0 ± 0.3
Blood glucose (mg/dl)	84.6 ± 6.0	90.0 ± 8.4	120.6 ± 21.7	125.4 ± 17.0
Insulin (ng/ml)	5.82 ± 1.16	4.47 ± 0.66	4.64 ± 2.70	14.50 ± 3.43*
Triglyceride (mg/dl)	60.7 ± 4.8	49.5 ± 4.6	45.2 ± 9.8	61.2 ± 4.1
Cholesterol (mg/dl)	87.4 ± 6.0	108.1 ± 5.0*	46.2 ± 6.4*	98.3 ± 5.3
NEFA (μEq/l)	0.92 ± 0.09	0.86 ± 0.01	0.94 ± 0.10	0.92 ± 0.04
Epididymal fat (mg)	115.8 ± 16.1	49.6 ± 2.6*	129.1 ± 29.9	404.6 ± 17.0*

n = 4–6.
* $p < 0.05$.

weeks of feeding are shown in Tables 3a and 3b, respectively. Body weights, glucose levels and lipid profiles at the beginning of the feeding period did not differ significantly among the groups (Table 3a). Body weights of the three different dietary groups did not differ significantly from that of the control group at the end of the 2-week feeding period, though the high-fat group tended to be heavier (Table 3b). Furthermore, the epididymal fat mass of the high-fat group was significantly larger than that of the control group at the end of the 2-week feeding period (C 115.8 ± 16.1 mg, HF 404.6 ± 17.0 mg; $p < 0.01$) (Table 3b). The high-carbohydrate group had a significantly reduced adipose tissue mass as compared to the control group (C 115.8 ± 16.1 mg, CA 49.6 ± 2.6 mg; $p < 0.05$) (Table 3b).

In contrast to the adipose depot mass, serum total cholesterol was slightly elevated in the high-carbohydrate group by the second week (C 87.4 ± 6.0 mg/dl, CA 108.1 ± 5.0 mg/dl; $p = 0.02$). The high-protein group, however, had significantly lower levels at the end of the second week (C 87.4 ± 6.0 mg/dl, P 46.2 ± 6.4 mg/dl; $p < 0.01$) (Table 3b). Serum non-esterified fatty acids (NEFA) and triglyceride levels did not differ significantly among the groups.

3.2. *Impaired glucose tolerance in the high-fat diet group*

To assess whether these diets impair glucose tolerance, intraperitoneal glucose tolerance tests were performed at the end of the 2-week feeding period, as described in Section 2 (Fig. 1). The high-fat group showed a significantly greater glucose rise than the control group, and showed this serum glucose elevation was sustained beyond the 120 min of the test. No such obvious glucose intolerance was detected in either the high-carbohydrate or the high-protein group.

3.3. *Expression levels of RELMβ and RELMγ in the colon, and of resistin and RELMα in white adipose tissue*

RELMβ expression profiles in fasted and fed states, and the correlations between levels in the colon and ileum are presented in Fig. 2. In the fasted state, the RELMβ protein level was downregulated 43.3 ± 17.2% as compared with that in the fed state (*ad libitum*), which suggests that the diet itself affects RELMβ expression (Fig. 2A and B). There was a positive correlation between RELMβ mRNA levels in the ileum and the colon ($r^2 = 0.604$, $p = 0.0002$), although the RELMβ mRNA level

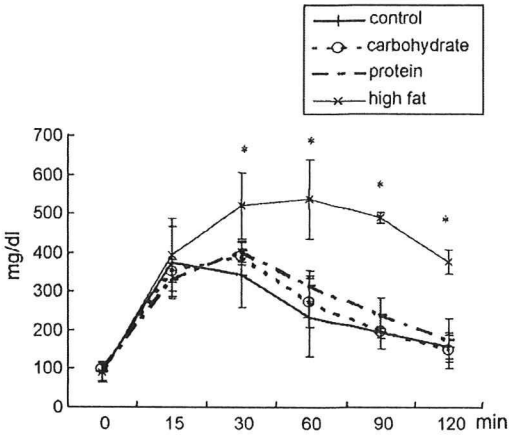

Fig. 1 – Impaired glucose tolerance in the high-fat diet group. The results of intra-peritoneal glucose tolerance tests done at the end of the second week are shown. Asterisks (*) denote glucose values significantly different from those of the control group. Bars indicate standard errors (n = 3–4).

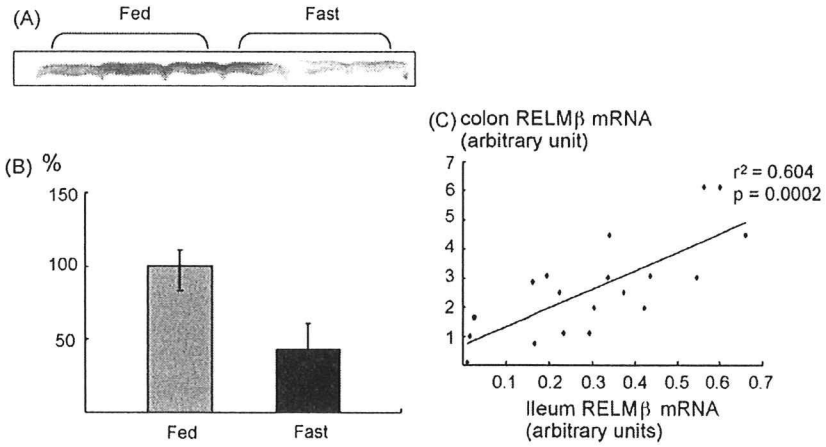

Fig. 2 – Altered expressions of RELMβ in fed and fasted states and comparison of RELMβ expressions in the ileum and colon. The protein level is shown as band (A), quantification as band (B), using NIH image. Asterisks (*) denote values in the state, which are significantly different from those in the fed state. Bars indicate standard errors ($n = 3$). The RELMβ mRNA level is shown in a scatter plot. The X-axis represents RELMβ from the ileum, the Y-axis that from the colon. Scales of the two are arbitrary but the values correspond to each other.

in the colon was more variable than that in the ileum, being up to 10 times higher (Fig. 2C). A positive correlation between RELMβ levels in serum and the colon was demonstrated previously [16].

As shown in Fig. 3A, interestingly, it was revealed that the high-carbohydrate and high-protein diets had markedly decreased RELMβ mRNA expression by the end of the 2-week feeding period (C 1.0 ± 0.34, CA 0.002 ± 0.001; $p = 0.02$, P 0.09 ± 0.06; $p < 0.01$) in the colon, while RELMβ mRNA expression in the high-fat group was slightly higher than that of the control group, but this difference was not statistically significant (Fig. 3A). In the ileum and serum, the same tendency was observed, as shown in Fig. 3B and C, although only serum RELMβ in the high protein group changed significantly (C 1.00 ± 0.15, CA 0.67 ± 0.33, P 0.46 ± 0.02, $p < 0.02$, F 1.31 ± 0.16 in serum, C 1.00 ± 0.24, CA 0.73 ± 0.10, P 0.68 ± 0.06, F 0.95 ± 0.23 in the ileum). These results suggest a strong influence of nutritional components on RELMβ expression in the colon. Furthermore, a single feeding produced no significant change in RELMβ mRNA (1.00 ± 0.13, CA 1.06 ± 0.23, P 0.84 ± 0.04 or F 0.82 ± 0.07) in the colon. The RELMβ mRNA level was changed by the diet itself, although repetitive and chronic stimulation was needed for those dietary components to change the RELMβ mRNA level.

The resistin mRNA analysis of white adipose tissue conducted during the second week of the feeding period, showed no significant differences among the groups (Fig. 4A). The RELMα mRNA expression levels in white adipose tissue

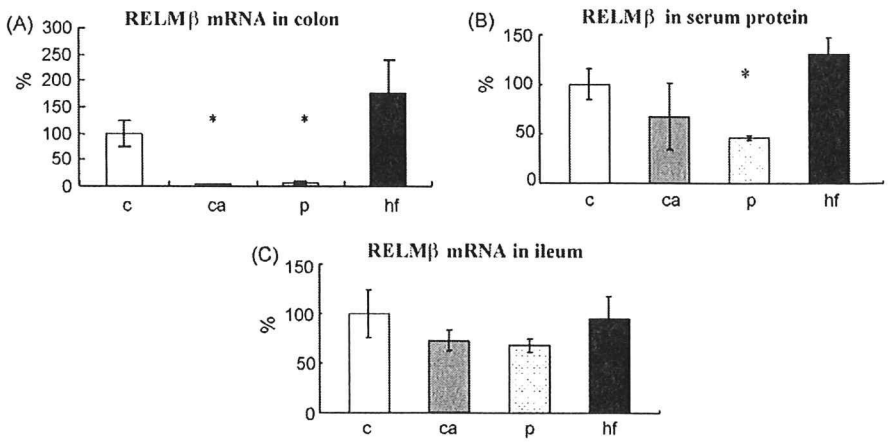

Fig. 3 – Altered expressions of RELMβ in the colon, ileum and serum in response to various dietary compositions. The mice were given a control, high-carbohydrate, high-protein or high-fat diet for 2 weeks. RELMβ expressions in the colon (A), serum (B) and ileum (C) were investigated and the data are presented as percentages of the control group values. Asterisks (*) denote values significantly different from those of the control group. Bars indicate standard errors ($n = 4$–6).

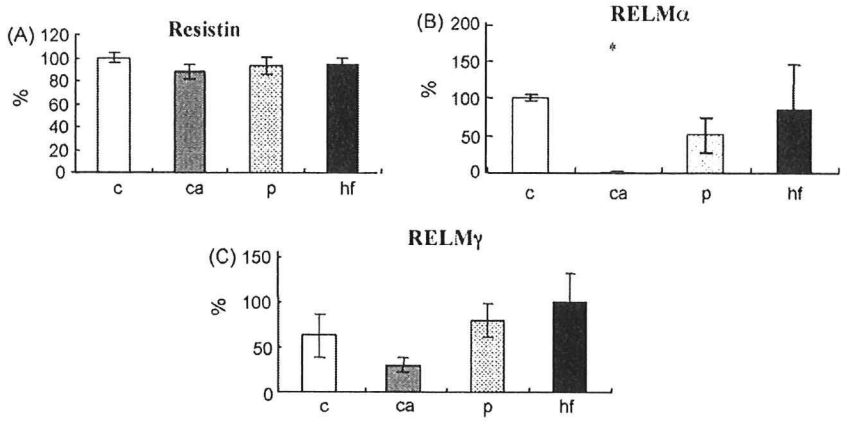

Fig. 4 – Expressions of resistin and RELMα mRNAs in adipose tissue and RELMγ in the colon in response to various dietary compositions. The mice were given a control, high-carbohydrate, high-protein or high-fat diet for 2 weeks. The expressions of resistin (A) and RELMα (B) mRNAs in adipose tissue and RELMγ (C) in the colon were investigated and the data are presented as percentages of the control group values. Asterisks (*) denote values significantly different from those of the control group. Bars indicate standard errors (n = 4–6).

are presented in Fig. 4B. RELMγ mRNA expressions in the colon did not differ among the dietary groups (Fig. 4C). Two-week feeding of a high-carbohydrate diet significantly suppressed RELMα expression as compared to the control group, while the high-protein and high-fat diets had no marked effects.

3.4. *Histological analysis*

Representative RELMβ immunohistochemistry of the colon, the major RELMβ production site, for each dietary group, is presented in Fig. 5. The high-carbohydrate and high-protein

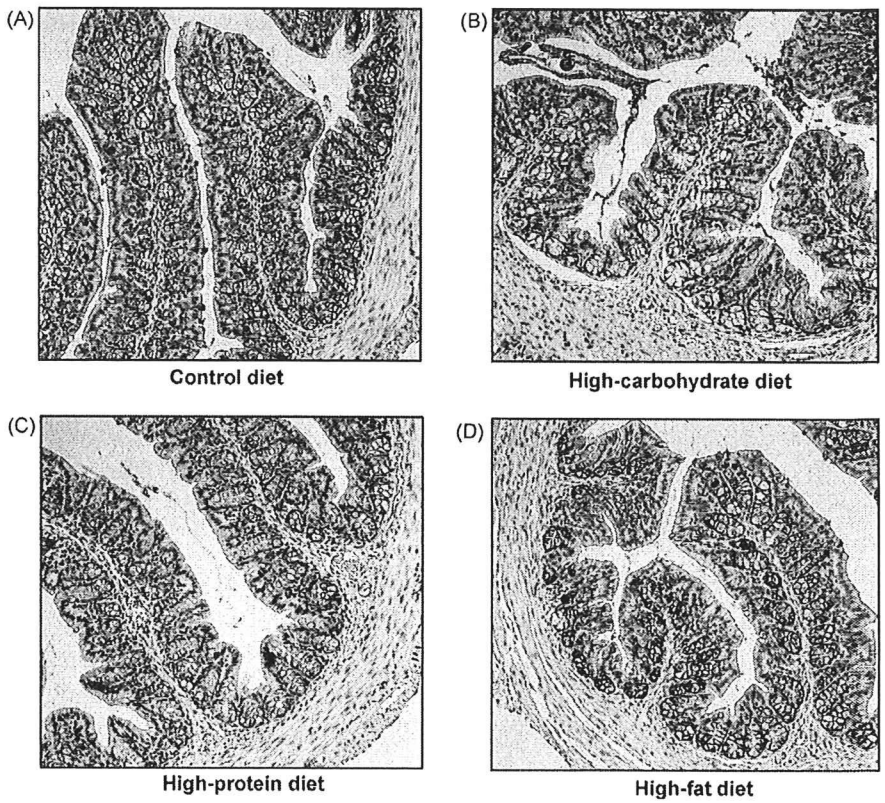

Fig. 5 – Colonic Immunohistochemistry of RELMβ. Colonic immunohistochemistry of RELMβ (magnification 100×) for each dietary group is shown. RELMβ is identifiable by its brown appearance. (A) Control diet, (B) high-carbohydrate diet, (C) high-protein diet, (D) high-fat diet.

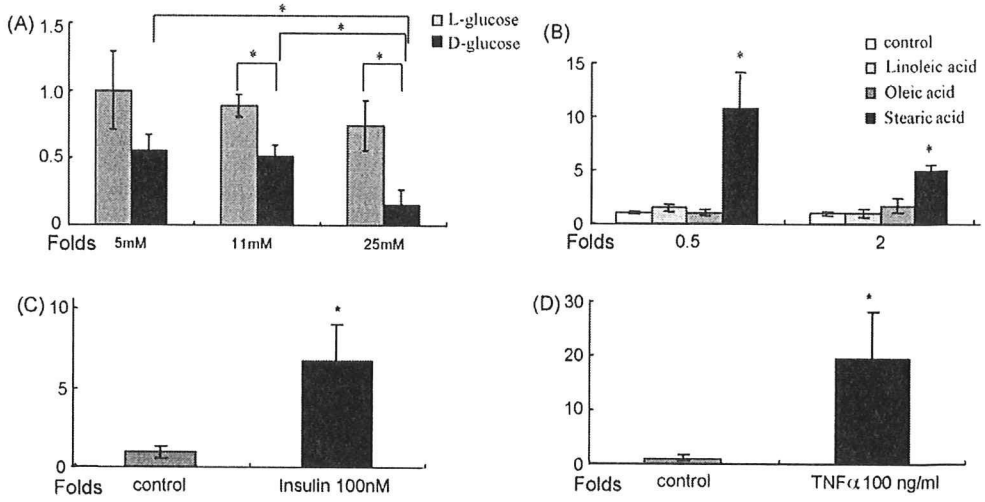

Fig. 6 – hRELMβ mRNA expression in LS174T cells with different stimuli. The hRELMβ mRNA expressions in LS174T cells after 24 h stimulation, with the agents shown at the indicated concentrations, are presented. (A) The cells were incubated with D-glucose or L-glucose at concentrations of 5 mM, 11 mM and 25 mM. The data are presented as the fold increase compared to the L-glucose group. (B) The cells were incubated with or without linoleic acid, oleic acid or stearic acid at concentrations of 0.5 and 2 mM. The data are shown as fold increases compared to the group without stimulation. (C) The cells were incubated with or without 100 nM insulin. (D) The cells were incubated with or without 100 ng/ml TNFα. Data from four separate experiments are presented and the bars indicate standard errors. The asterisks (*) denote values significantly different from those of the control group.

diet groups showed significantly less RELMβ expression than the control and high-fat diet groups. HE-stained preparations from all dietary groups were compared for the number of goblet cells. The absence of significant differences in numbers of intestinal goblet cells, among the groups, was also confirmed.

3.5. *Changes in hRELMβ mRNA expression in a human colon cancer cell line with various stimulations*

Expressions of hRELMβ mRNA in the human colon cancer cell line LS174T, were compared after stimulation with D-glucose or L-glucose, insulin, TNFα and three types of FFA, as described in Section 2. The results are presented in Fig. 6. Stimulation with D-glucose at 5, 11 and 25 mM significantly reduced the RELMβ mRNA expression in a concentration dependent manner (Fig. 6A). The three FFA exerted different effects on mRNA expression. Stearic acid stimulation resulted in marked upregulation of the RELMβ mRNA level (0.5 mM stearic acid, 10.7 ± 3.3 fold; $p < 0.01$, 2.0 mM stearic acid, 3.4 ± 0.38 fold; $p < 0.01$), while linoleic and oleic acids had no significant effects (Fig. 6B).

Stimulation with 100 nM insulin induced a 6.7-fold increase in mRNA expression ($p < 0.01$) (Fig. 6C). TNFα stimulation markedly increased RELMβ mRNA expression, by approximately 20 fold ($p < 0.01$) (Fig. 6D).

4. Discussion

One major factor contributing to Type 2 diabetes mellitus is insulin resistance, and obesity is known to be the most common factor inducing insulin resistance. Pathophysiological states (*i.e.* insulin resistance, obesity, and low-grade inflammation) are major and synergistic components of the metabolic syndrome. It was recently demonstrated that adipocytes are not only a lipid depot site, but also actively produce and secrete hormones and cytokines [19]. Resistin is one of these adipocyte-derived proteins and was suggested to play a role in the development of insulin resistance [4].

In addition, it was revealed that resistin and three structurally related RELMs constitute a resistin family [2,3,14]. Only RELMβ among these three RELMs is present in humans. Intestinal RELMβ secretion is reportedly increased in response to bacterial colonization [14] and has been suggested to be involved in the defense mechanism against nematode infestation in mice [15]. On the other hand, administration of RELMβ via the bloodstream induces acute hepatic insulin resistance [20], and transgenic mice over-expressing RELMβ in the liver were shown to exhibit hyperglycemia, hyperlipidemia and fatty liver [17]. These findings suggest that RELMβ is involved in both inflammatory responses intrinsic to the intestine and insulin resistance, particularly in the liver, and therefore may be an important link between these two pathophysiological states. Taking the aforementioned background factors into consideration, we carried out this study to investigate the regulatory effects of various nutritional factors in food on the expressions of RELMβ and other isoforms.

The effects of different nutritional components of diets are now receiving attention, especially in relation to obesity. With the intention of preventing and treating obesity and related diseases, intervention trials have been undertaken [21,22]. Diets rich in carbohydrate and low in fat have been employed, and have been found to reduce the incidence of diabetes by up

to 60%. Diets of similar composition are also recommended by medical societies for the treatment of diabetes [23,24]. Another study revealed that a high-protein diet resulted in substantial and sustained improvements in waist circumference, triglycerides and insulin, whereas with a high carbohydrate diet these changes were more modest [25]. In patients with Type 2 diabetes, a high protein diet reportedly improved glucose metabolism, due to the stimulatory effect of protein on insulin secretion [26].

In the present study, neither the high-carbohydrate nor the high-protein diet for 2 weeks induced either hyperinsulinemia or hyperglycemia in the fasting condition, nor was there any obvious glucose tolerance impairment in mice. Furthermore, epididymal fat tissue masses in both groups were reduced or were similar to those of the control group. These results are in a good accordance with the reported observations in a clinical trial [25]. In this study, we first demonstrated RELMβ expression in mice to be strongly influenced by whether the animals were fasted or fed, and differences in dietary nutritional composition, while resistin expression in adipose tissues did not differ significantly among the dietary groups. Resistin levels in white adipose tissue are reportedly higher in insulin resistant rodent models [4], though others have described contrasting observations [6–8]. Post-transcriptional and/or post-translational modifications, that consequently affect the secretion rate of the protein, have been suggested as possible explanations for this discrepancy.

Since RELMβ is the only RELM in humans, we focused on the regulation of colonic RELMβ expression, which was significantly suppressed in both the high-protein and the high-carbohydrate group. The histological investigations ruled out suppressed RELMβ expression due to a reduced number of goblet cells, and indicated that RELMβ secretion is markedly influenced by nutrients. Therefore, we speculate that protein and carbohydrate exert suppressive effects, or alternatively that an as yet unknown lipid, induces RELMβ expression. We also considered the possible involvement of insulin and TNFα, serum concentrations of which are increased in high-fat diet-induced insulin resistance. To examine these possibilities, a human colon cancer cell line, LS174T, which has been shown to express human RELMβ (RELMβ) under basal conditions [14], was subjected to various culture conditions. The initial incubation of these cells with D-glucose induced significantly lower RELMβ expression, in a D-glucose concentration dependent manner, than the same L-glucose concentrations. Subsequently, it was revealed that only the saturated FFA, *i.e.* stearic acid, had significant inducing effects on RELMβ mRNA expression, while the other two free fatty acids had little impact.

We also demonstrated insulin and TNFα to markedly increase RELMβ expression. Induction of RELMβ expression by TNFα is an observation in good accordance with previous study results showing induction of RELMβ expression by Th2 cytokines such as Il-4 and IL-13 [15]. Furthermore, the presence of several STAT6 and NFκB elements in the promoter region of human RELMβ was disclosed by sequence analysis [14].

Taking these results together, we can suggest possible mechanisms underlying diet-induced RELMβ regulation. First, repetitive and chronic stimulation by certain free fatty acids, such as stearic acid, or glucose, *per se*, increased and decreased RELMβ expression, respectively. Second, although no supporting data were obtained in this study, it is reasonable to speculate that the different nutritional compositions of foods would affect bacterial colonization in the colon, and that differences in bacterial colonization might affect RELMβ expression either directly or indirectly (*i.e.* systemic hormonal changes) through local Th2 cytokine production. Finally, a high-fat diet enlarges adipocytes, which in turn induces the secretion of various proteins such as TNFα while high-carbohydrate and high-protein diets reduce adipocyte size. In addition, FFA also reportedly induces the release of TNFα from macrophages [27]. TNFα secreted by adipocytes and macrophages would then induce the expression of RELMβ. We speculate that some or all of these mechanisms are involved in the nutrient-induced regulation of RELMβ. The high concentrations of RELMβ secreted by the intestines would reach the liver via the blood stream and thus contribute to the development of insulin resistance.

In conclusion, this study has clearly shown intestinal RELMβ expression to be strongly influenced by the nutritional compositions of foods. Up-regulation by inflammatory mediators, together with the previous demonstration of the RELMβ association with insulin resistance, suggests a role for this protein as a cytokine contributing to the pathogenesis of insulin resistance and thereby to that of the metabolic syndrome.

REFERENCES

[1] C.M. Steppan, E.J. Brown, C.M. Wright, S. Bhat, R.R. Banerjee, C.Y. Dai, et al., A family of tissue-specific resistin-like molecules, Proc. Natl. Acad. Sci. U.S.A. 98 (2001) 502–506.
[2] B. Gerstmayer, D. Kusters, S. Gebel, T. Muller, E. Van Miert, K. Hofmann, et al., Identification of RELMgamma, a novel resistin-like molecule with a distinct expression pattern, Genomics 81 (2003) 588–595.
[3] I.N. Holcomb, R.C. Kabakoff, B. Chan, T.W. Baker, A. Gurney, W. Henzel, et al., FIZZ1, a novel cysteine-rich secreted protein associated with pulmonary inflammation, defines a new gene family, EMBO J. 19 (2000) 4046–4055.
[4] C.M. Steppan, S.T. Bailey, S. Bhat, E.J. Brown, R.R. Banerjee, C.M. Wright, et al., The hormone resistin links obesity to diabetes, Nature 409 (2001) 307–312.
[5] R.R. Banerjee, S.M. Rangwala, J.S. Shapiro, A.S. Rich, B. Rhoades, Y. Qi, et al., Regulation of fasted blood glucose by resistin, Science 303 (2004) 1195–1198.
[6] J.M. Way, C.Z. Gorgun, Q. Tong, K.T. Uysal, K.K. Brown, W.W. Harrington, et al., Adipose tissue resistin expression is severely suppressed in obesity and stimulated by peroxisome proliferator-activated receptor gamma agonists, J. Biol. Chem. 276 (2001) 25651–25653.
[7] G. Milan, M. Granzotto, A. Scarda, A. Calcagno, C. Pagano, G. Federspil, et al., Resistin and adiponectin expression in visceral fat of obese rats: effect of weight loss, Obes. Res. 10 (2002) 1095–1103.
[8] C.C. Juan, L.C. Au, V.S. Fang, S.F. Kang, Y.H. Ko, S.F. Kuo, et al., Suppressed gene expression of adipocyte resistin in an insulin-resistant rat model probably by elevated free fatty acids, Biochem. Biophys. Res. Commun. 289 (2001) 1328–1333.
[9] I. Nagaev, U. Smith, Insulin resistance and type 2 diabetes are not related to resistin expression in human fat cells or

skeletal muscle, Biochem. Biophys. Res. Commun. 285 (2001) 561–564.
[10] K.H. Kim, K. Lee, Y.S. Moon, H.S. Sul, A cysteine-rich adipose tissue-specific secretory factor inhibits adipocyte differentiation, J. Biol. Chem. 276 (2001) 11252–11256.
[11] T. Liu, H. Jin, M. Ullenbruch, B. Hu, N. Hashimoto, B. Moore, et al., Regulation of found in inflammatory zone 1 expression in bleomycin-induced lung fibrosis: role of IL-4/IL-13 and mediation via STAT-6, J. Immunol. 173 (2004) 3425–3431.
[12] A.M. Chumakov, T. Kubota, S. Walter, H.P. Koeffler, Identification of murine and human XCP1 genes as C/EBP-epsilon-dependent members of FIZZ/resistin gene family, Oncogene 23 (2004) 3414–3425.
[13] T. Schinke, M. Haberland, A. Jamshidi, P. Nollau, J.M. Rueger, M Amling, Cloning and functional characterization of resistin-like molecule gamma, Biochem. Biophys. Res. Commun. 314 (2004) 356–362.
[14] W. He, M.L. Wang, H.Q. Jiang, C.M. Steppan, M.E. Shin, M.C. Thurnheer, et al., Bacterial colonization leads to the colonic secretion of RELMbeta/FIZZ2, a novel goblet cell-specific protein, Gastroenterology 125 (2003) 1388–1397.
[15] D.W.M. Artis, S.A. Keilbaugh, W. He, M. Brenes, G.P. Swain, P.A. Knight, D.D. Donaldson, et al., RELMbeta/FIZZ2 is a goblet cell-specific immune-effector molecule in the gastrointestinal tract, Proc. Natl. Acad. Sci. U.S.A. 101 (2004) 13596–13600.
[16] N. Shojima, T. Ogihara, K. Inukai, M. Fujishiro, H. Sakoda, A. Kushiyama, et al., Serum concentrations of resistin-like molecules beta and gamma are elevated in high-fat-fed and obese db/db mice, with increased production in the intestinal tract and bone marrow, Diabetologia 48 (2005) 984–992.
[17] A. Kushiyama, N. Shojima, T. Ogihara, K. Inukai, H. Sakoda, M. Fujishiro, et al., Resistin like molecule beta activates MAPKs, suppresses insulin signaling in hepatocytes and induces diabetes, hyperlipidemia and fatty liver in transgenic mice on a high-fat diet, J. Biol. Chem. 280 (2005) 42016–42025.
[18] S.R. Krutzik, M.T. Ochoa, P.A. Sieling, S. Uematsu, Y.W. Ng, A. Legaspi, et al., Activation and regulation of Toll-like receptors 2 and 1 in human leprosy, Nat. Med. 9 (2003) 525–532.
[19] B.B. Kahn, J.S. Flier, Obesity and insulin resistance, J. Clin. Invest. 106 (2000) 473–481.
[20] M.W. Rajala, S. Obici, P.E. Scherer, L. Rossetti, Adipose-derived resistin and gut-derived resistin-like molecule-beta selectively impair insulin action on glucose production, J. Clin. Invest. 111 (2003) 225–230.
[21] J. Tuomilehto, J. Lindstrom, J.G. Eriksson, T.T. Valle, H. Hamalainen, P. Ilanne-Parikka, et al., Prevention of type 2 diabetes mellitus by changes in lifestyle among subjects with impaired glucose tolerance, N. Engl. J. Med. 344 (2001) 1343–1350.
[22] W.C. Knowler, E. Barrett-Connor, S.E. Fowler, R.F. Hamman, J.M. Lachin, E.A. Walker, et al., Reduction in the incidence of type 2 diabetes with lifestyle intervention or metformin, N. Engl. J. Med. 346 (2002) 393–403.
[23] M.J. Franz, J.P. Bantle, C.A. Beebe, J.D. Brunzell, J.L. Chiasson, A. Garg, et al., Evidence-based nutrition principles and recommendations for the treatment and prevention of diabetes and related complications, Diabetes Care 26 (Suppl. 1) (2003) S51–S61.
[24] The Diabetes and Nutrition Study Group (DNSG) of the European Association for the Study of Diabetes (EASD), 1999, Recommendations for the nutritional management of patients with diabetes mellitus, Eur. J. Clin. Nutr. 54 (2000) 353–355.
[25] K.A. McAuley, K.J. Smith, R.W. Taylor, R.T. McLay, S.M. Williams, J.I. Mann, Long-term effects of popular dietary approaches on weight loss and features of insulin resistance, Int. J. Obes. (Lond) (2005) 342–349.
[26] F.Q. Nuttall, M.C. Gannon, Metabolic response of people with type 2 diabetes to a high protein diet, Nutr. Metab. (Lond) 1 (2004) 6.
[27] T.N.J. Suganami, Y. Ogawa, A paracrine loop between adipocytes and macrophages aggravates inflammatory changes: role of free fatty acids and tumor necrosis factor-alpha, Arterioscler. Thromb. Vasc. Biol. 25 (2005) 2062–2068.

ORIGINAL ARTICLE

Adiponectin Upregulates Ferritin Heavy Chain in Skeletal Muscle Cells

Yuichi Ikegami,[1] Kouichi Inukai,[1] Kenta Imai,[1] Yasushi Sakamoto,[2] Hideki Katagiri,[3] Susumu Kurihara,[1] Takuya Awata,[1] and Shigehiro Katayama[1]

OBJECTIVE—Adiponectin is an adipocyte-derived protein that acts to reduce insulin resistance in the liver and muscle and also inhibits atherosclerosis. Although adiponectin reportedly enhances AMP-activated protein kinase and inhibits tumor necrosis factor-α action downstream from the adiponectin signal, the precise physiological mechanisms by which adiponectin acts on skeletal muscles remain unknown.

RESEARCH DESIGN AND METHODS—We treated murine primary skeletal muscle cells with recombinant full-length human adiponectin for 12 h and searched, using two-dimensional electrophoresis, for proteins upregulated more than threefold by adiponectin compared with untreated cells.

RESULTS—We found one protein that was increased 6.3-fold with adiponectin incubation. MALDI-TOF (matrix-assisted laser desorption/ionization–top of flight) mass spectrometric analysis identified this protein as ferritin heavy chain (FHC). When murine primary skeletal muscle cells were treated with adiponectin, IκB-α phosphorylation was observed, suggesting that adiponectin stimulates nuclear factor (NF)-κB activity. In addition, FHC upregulation by adiponectin was inhibited by NF-κB inhibitors. These results suggest NF-κB activation to be involved in FHC upregulation by adiponectin. Other NF-κB target genes, manganese superoxide dismutase (*MnSOD*) and inducible nitric oxide synthase (*iNOS*), were also increased by adiponectin treatment. We performed a reactive oxygen species (ROS) assay using CM-H_2DCFDA fluorescence and found that ROS-reducing effects of adiponectin were abrogated by FHC or MnSOD small-interfering RNA induction.

CONCLUSIONS—We have demonstrated that adiponectin upregulates FHC in murine skeletal muscle tissues, suggesting that FHC elevation might partially explain how adiponectin protects against oxidative stress in skeletal muscles. ***Diabetes* 58:61–70, 2009**

Adipocytes have been recognized to secrete a variety of proteins, such as tumor necrosis factor (TNF)-α, adipsin, plasminogen activator inhibitor-1, leptin, resistin, and adiponectin. These proteins are termed adipokines and are likely to physiologically exert a variety of hormonal actions (1). Among these proteins, adiponectin is exclusively expressed in adipose tissue and consists of an NH_2-terminal collagenous domain and a COOH-terminal globular domain (2). Adiponectin belongs to the soluble collagen superfamily and has structural homology with collagens VIII and X, complement factor C1q (3), and the TNF family (2,4). Circulating adiponectin is extremely abundant (~15 μg/ml), and adiponectin forms various oligomeric complexes, including low (LMW), medium (MMW), and high (HMW) molecular weight species. Adiponectin exerts antidiabetes effects on muscles and the liver through AMP-activated protein kinase activation (5) and antiatherosclerotic effects by inhibiting monocyte adhesion to endothelial cells and lipid accumulation into macrophages (6,7). Thus, adiponectin increases glucose uptake and fatty acid oxidation in muscles via the type 1 adiponectin receptor (8), and decreases hepatic gluconeogenesis via the type 2 adiponectin receptor (8,9). On the other hand, nuclear factor (NF)-κB but not AMP-activated protein kinase activity was demonstrated to be enhanced by MMW or HMW adiponectin in muscles (10). According to recent studies (9–14), HMW adiponectin appears to be more important for the antidiabetes and antiatherosclerotic effects than the other two oligomeric complexes. Though the physiological role of HMW adiponectin in improving insulin resistance or reducing oxidative stress is clearly significant, the precise mechanisms by which adiponectin acts on skeletal muscles remain unknown.

Therefore, in the present study, we investigated adiponectin function in primary cultured skeletal muscle cells by comparing protein expressions in untreated cells using two-dimentional electrophoresis. A marked increase in FHC protein was observed with adiponectin incubation. FHC is one of two subunits of ferritin, the other being ferritin light chain (FLC) (15), and has ferroxidase activity, which is required for iron sequestration (16). FHC was reported to suppress reactive oxygen species (ROS) production (17), which may explain the ROS-reducing effects of adiponectin. FHC upregulation followed by an enhanced ROS-reducing effect is suggested to be a novel mechanism by which adiponectin acts directly against oxidative stress.

RESEARCH DESIGN AND METHODS

Cell culture and chemicals. Murine primary cultured skeletal muscle cells were purchased from Cell Garage (Tokyo, Japan) in cultured flasks, and maintained in DMEM containing 10% fetal bovine serum (FBS). We switched the medium to DMEM containing 2% horse serum, which promotes differentiation of myocytes into myotubes, and continued the incubation for 5 days before the experiments. Human umbilical vein endothelial cells (HUVECs) were purchased from Cambrex (Baltimore, MD) as cryopreserved cells. After thawing, the cells were plated in collagen-coated culture flasks and cultured to confluence in EBM-2 medium (Lonza, Walkersville, MD) containing the indicated ligands, 2% FBS, and antibiotics (BulletKit EGM-2, cat. no. CC-3162). C2C12 myoblasts were maintained in DMEM containing 10% FBS at 37°C in 5%

From the [1]Department of Endocrinology and Diabetes, School of Medicine, Saitama Medical University, Saitama, Japan; the [2]Division of Analytical Science, Department of Biochemical Research Center, Saitama Medical University, Saitama, Japan; and the [3]Division of Molecular Metabolism and Diabetes, Tohoku University Graduate School of Medicine, Miyagi, Japan.
Corresponding author: Kouichi Inukai, inukai@saitama-med.ac.jp.
Received 25 May 2007 and accepted 8 October 2008.
Published ahead of print at http://diabetes.diabetesjournals.org on 17 October 2008. DOI: 10.2337/db07-0690.

CO_2. After the C2C12 cells reached subconfluence, differentiation was induced by treatment with DMEM containing 5% horse serum for 7 days, at which time formation of myotubes was maximal. The following chemicals were purchased: H89 from Seikagaku (Tokyo, Japan); NF-κB inhibitor, NF-κB SN50, and BAY11-7082 from Biomol Research Laboratories (Plymouth Meeting, PA); forskolin, TNF-α, palmitate, and iron (II) sulfate heptahydrate from Sigma-Aldrich (St. Louis, MO); human recombinant adiponectin from R&D Systems (Minneapolis, MN); human recombinant globular adiponectin from BioVendor Laboratory Medicine (Modrice, Czech Republic); and 4-hydroxynonenal from Calbiochem (San Diego, CA). Fatty acid solution was prepared by a method described previously (18).

Two-dimensional electrophoresis. A total of 3.0×10^6 murine primary cultured skeletal muscle cells were dissolved in lysis solution (7 mol/l urea, 2 mol/l thiourea, 4% CHAPS, 0.5% IPG buffer, 18 mmol/l dithiothreitol, and 2 mmol/l phenylmethanesulphonylfluoride, pH 8.5). Impurities such as salts, lipids, detergent, and nucleic acids were then removed from samples using a two-dimensional clean-up kit (Amersham Pharmacia Biotech, Amersham, U.K.). Samples were redissolved in rehydration solution and centrifuged at 24,000 rpm for 20 min at 10°C, and insoluble substances were removed. Using 450 μl of solution corresponding to 400 μg of murine primary cultured skeletal muscle cell protein, two-dimensional gel electrophoresis was performed according to the manufacturer's instructions (Amersham Pharmacia Biotech). The gels were Coomassie brilliant blue stained using PhastGel Blue R-350. Colloidal Coomassie blue–stained gels were scanned using a GS-800 calibrated densitometer (Bio-Rad Laboratories, Hercules, CA), and gel images were analyzed using PDQuest 2D-Image-Analysis software (version 7.3; Bio-Rad Laboratories). For this analysis, three independent sets consisting of a control sample gel and an adiponectin-treated sample gel were prepared. For a between-gel comparison, a set of spot-generation conditions was used. To analyze the proteins, we first chose one protein signal to assure that the number of proteins, with signals more intense than that initially chosen, would be ~1,500. Then, we analyzed only these 1,500 protein signals. The computer allowed automatic detection and quantification of protein spots, as well as matching between the control and adiponectin-treated gels. Routine statistical analysis available within the software package was used to identify up- or down-expressed spots. The differentially expressed protein spots were identified by quantitative comparisons with control gels.

Identification of proteins upregulated by adiponectin. Protein spots of interest were excised from the gels and subjected to matrix-assisted laser desorption/ionization–top of flight (MALDI-TOF) mass spectrometry. In-gel digestion of the individual protein spots was done by the following method. Pieces of gel were destained using 200 μl of 50 mmol/l ammonium bicarbonate in 50% acetonitrile, dehydrated in 200 μl of acetonitrile, and then completely dried by vacuuming and centrifuging. The samples were then allowed to expand in digestion buffer containing 100 mmol/l ammonium bicarbonate, 20 μg/ml of trypsin (Promega, Madison, WI), and 0.1% octyl β-D-glucopyranoside (Sigma-Aldrich) at 4°C. After a 30-min incubation, the samples were incubated overnight at 37°C. Peptides were then extracted twice using 0.1% trifluoroacetic acid in 30% acetonitrile with sonication. The peptide solution was vacuum concentrated until it had decreased to 10 μl and desalted according to the manufacturer's protocol. An AXIMA-CFR model MALDI-TOF mass spectrometer (Shimadzu, Kyoto, Japan) was used for mass analysis of tryptic peptide mixtures. Peptides were identified with the Mascot search program (Matrix Science, London, U.K.).

Western blotting and quantitative PCR. Western blotting was performed as previously described (19). Briefly, after incubation with the indicated chemicals, primary cultured skeletal muscle cells were washed with ice-cold PBS, lysed in ice-cold lysis buffer, and then centrifuged at 14,000*g* for 10 min at 4°C. Supernatants including tissue protein extracts were resolved on 10% SDS-PAGE, followed by electrophoretic transfer to a nitrocellulose membrane. Membranes were incubated for 1 h at room temperature with the appropriate primary antibody. Commercial antibodies against phosphor–inhibitor of κB-α (IκB-α), intercellular adhesion molecule (ICAM)-1 FHC FLC, p65 NF-κB (Santa Cruz Biotechnology, Santa Cruz, CA), and IκB-α (Cell Signaling Technology, Palo Alto, CA) were purchased. After blotting with the indicated secondary antibody, detection was performed using an ECL chemiluminescent kit (Amersham Pharmacia Biotech), according to the manufacturer's instructions. Quantitations were performed using a Molecular Imager (Bio-Rad Laboratories). cDNA was synthesized from the purified total RNA using a reverse transcriptase kit (Amersham Pharmacia Biotech), according to the manufacturer's instructions. For quantitative analysis of FHC, manganese superoxide dismutase (MnSOD), and inductible nitric oxide synthase (iNOS), we conducted real-time PCR using an ABI PRISM model 7000 (Applied Biosystems, Foster City, CA), according to the manufacturer's instructions. The primer sets and probes for murine FHC (assay ID: Mm00850707_g1), murine MnSOD (assay ID: Mm00449726_m1), and murine iNOS (assay ID: Mm00440485_m1) were purchased. Nuclear protein extracts were prepared by separating the cell pellet into two compartments (i.e., the nucleus and the cytosol), as previously described (18).

Small-interfering RNA reagents and transfection. C2C12 myotubes were transfected with small-interfering (siRNA) against FHC (ID 158606, 66945), MnSOD (ID 152022, 71294), and iNOS (ID 156550, 68442) (Applied Biosystems) using the transfection reagent (AM4510; Applied Biosystems), following the manufacturer's protocol. As the control, we utilized the commercially available siRNA control nonsilencing sequence (4611G; Applied Biosystems). The cells were used for experiments 48 h after siRNA transfection.

Generation and transfection of recombinant adenoviruses expressing FHC and adiponectin. A full-length mouse FHC cDNA was isolated from mouse hepatic RNA by reverse-transcriptase PCR. The oligonucleotide sequences used for PCR were as follows: coding strand, 5′-ACCATGACCACCGCGTCTCCCTCGCAAGTG-3′; noncoding strand, 5′-AGCTTAGCTCTCATCACCGTGTCCCAGGGT-3′. The cDNA was subcloned into TA vectors, pCRII (Invitrogen Life Technologies, CA), sequenced to confirm their identities, and were observed to have no unexpected mutations. Adenovirus-expressing recombinant FHC was prepared by homologous recombination of the expression cosmid cassettes containing the corresponding cDNAs and the parental adenovirus genome, as described previously (20). Adenovirus-expressing recombinant adiponectin was prepared as reported previously (21). For adenovirus-mediated transfection, cultured cells were incubated for 2 h in 37°C with DMEM containing the adenovirus-expressing LacZ or FHC, and the growth media were then added. Experiments were performed 3 days after transfection. Mice were treated with recombinant adenovirus, expressing LacZ or adiponectin, by systemic injection into the tail vein.

Assay of intracellular cAMP contents. cAMP was measured in murine primary cultured skeletal muscle cells using a direct enzyme immunoassay kit according to the instructions provided by the manufacturer (Amersham Pharmacia Biotech). Briefly, cell lysates (100 μl) were transferred to a new 96-well microplate coated with donkey anti-rabbit IgG. After addition of 100 μl of rabbit anti-cAMP serum to each well, the microplate contents were gently mixed and incubated at 4°C for 2 h. Then, after addition of 50 μl of cAMP peroxidase conjugate to each well, the microplates were gently agitated and incubated at 4°C for 60 min. We aspirated and washed each well four times with 400 μl of washing buffer and blotted the plate on tissue paper to remove any residual liquid. Next, we immediately dispensed 150 μl of enzyme substrate into each well, followed by mixing on a microplate shaker for exactly 60 min at room temperature. To halt the reaction, we added 100 μl of 1.0 mol/l sulfuric acid to each well. The optical density was determined in a plate reader at 450 nm.

Detection of intracellular ROS production. Intracellular ROS production was monitored by flow cytometry (Becton Dickinson, Franklin Lakes, NJ) using 5-(and 6)-chloromethyl-2′,7′-dichlorodihydrofluorescein diacetate, acetyl ester (CM-H_2DCFDA). Cells were stimulated with the indicated reagents in culture dishes and incubated for 24 h. Then, these cells were washed twice in PBS, followed by addition of 10 μmol/l CM-H_2DCFDA in PBS, and finally placed in the dark at 37°C for 1 h. The cells were washed once, harvested, and suspended in 500 μl PBS. Dead cells were excluded by adding 10 μmol/l propidium iodide, a nuclear stain to which viable cells are impermeable. ROS levels were measured by flow cytometrically by determining the mean fluorescent intensity relative to that of the control group. Using this method, we were able to measure not only H_2O_2 but also hydroxy radical ($^{\cdot}$OH) or peroxynitrite ($ONOO^-$). As it was important to measure hydroxy radicals (OH), generated by the Fenton reaction, we adopted this method.

Animals. Nine-week-old male mice (C57BL/KsJ, $n = 14$) were purchased from Clea Japan (Osaka, Japan). After a 2- to 3-day acclimatization period, all mice were maintained on a 12:12-h light-dark cycle, fed a standard rodent diet ad libitum, and given unlimited access to water. The mice were divided into a LacZ-transferred group (control construct) and an adiponectin-transferred group (adiponectin construct), and adenovirus-mediated gene transfer was performed. Before they were killed, the animals were fasted for 8 h. Three days after virus infection, increased serum adiponectin levels were confirmed using both a mouse/rat adiponectin ELISA kit (Otsuka, Tokushima, Japan) and immunoblot analysis with anti-murine adiponectin antibody (Chemicon International, Temecula, CA). Then, total hind limbs were removed and immediately homogenized with a Polytron homogenizer in six volumes of solubilization buffer. Extracts were centrifuged at 15,000*g* for 30 min at 4°C, and the supernatants were used as samples for immunoblotting with anti-FHC antibody.

Statistical analysis. All data were expressed as means ± SE. The statistical significance of differences between groups was assessed with the unpaired Student's *t* test using Stat View software (version 5.01; SAS Institute, Cary, NC). A P value <0.05 was considered statistically significant.

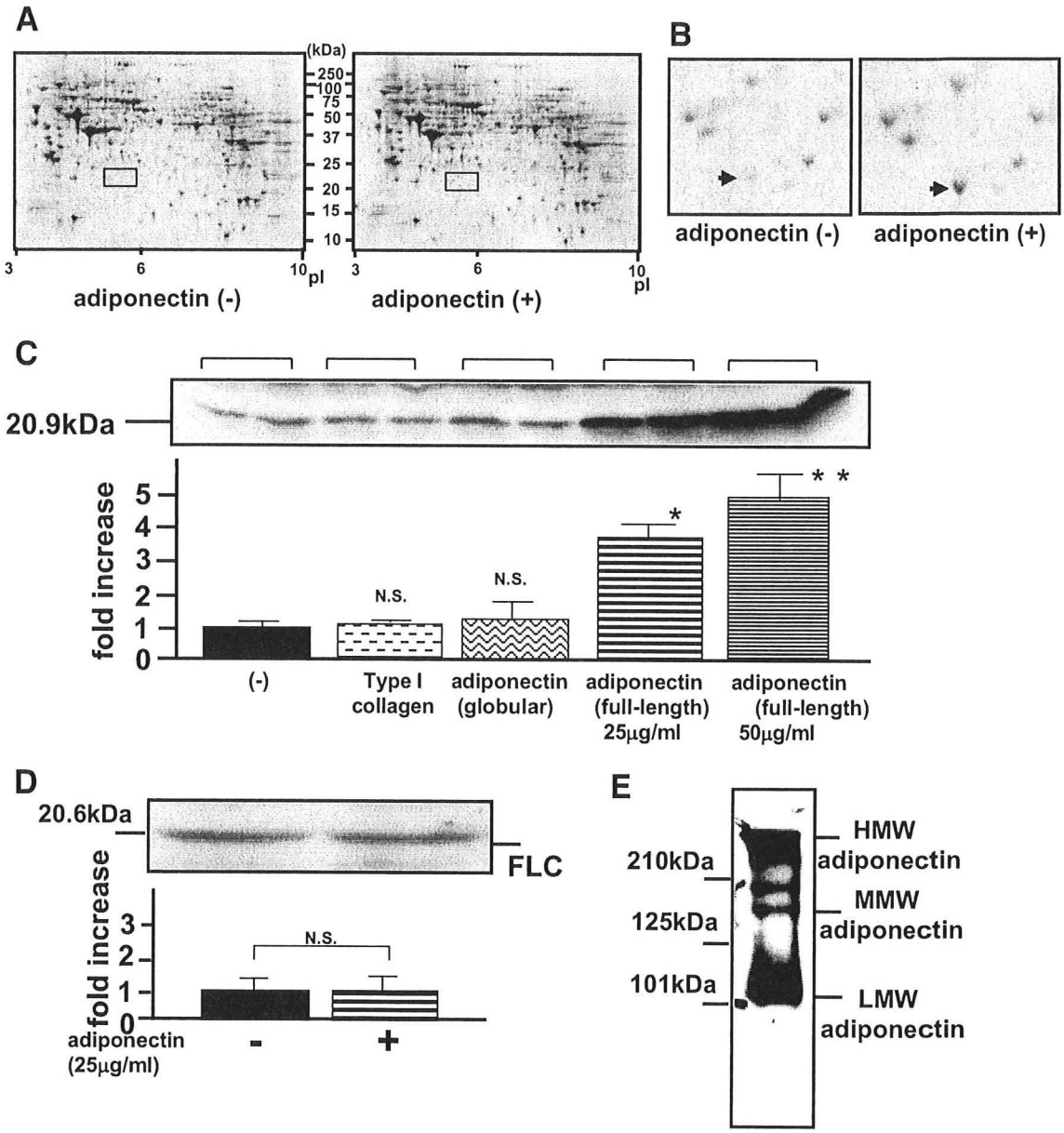

FIG. 1. Effects of incubation with HMW adiponectin on primary cultured skeletal muscles. Primary cultured murine skeletal muscles were incubated for 12 h in the presence (+) or absence (−) of adiponectin (25 μg/ml). *A*: Whole images of Coomassie brilliant blue–stained gels for two-dimensional electrophoresis in the absence (*left*) or presence (*right*) of adiponectin. *B*: Magnified images of two-dimensional electrophoresis revealing a spot apparently altered by adiponectin treatment (arrows). Three two-dimensional electrophoresis sets yielded similar results. *C–E*: After incubation with the indicated ligands, primary cultured skeletal muscle cells were lysed in ice-cold lysis buffer and centrifuged at 14,000*g* for 10 min at 4°C. Supernatants including tissue protein extracts were resolved on 10% SDS-PAGE, followed by electrophoretic transfer to a nitrocellulose membrane. Membranes were incubated for 1 h at room temperature with antibody against mouse FHC (*C*) or FLC (*D*). *E*: The recombinant full-length human adiponectin, which was expressed in a mouse myeloma cell line NS0, was resolved on 7.5% SDS-PAGE under nonreducing conditions and investigated by immunoblotting with anti-adiponectin antibody. After blotting with the indicated secondary antibody, detection was performed using an electrochemiluminescence chemiluminescent kit according to the manufacturer's instructions. Representative data from four independent experiments are presented. *Significant difference ($P < 0.05$) relative to FHC expression in control cells. **Significant difference ($P < 0.05$) relative to FHC expression with 25 μg/ml of adiponectin. N.S., not significant relative to control cells in the absence of adiponectin.

RESULTS

Identification of proteins upregulated by adiponectin. We treated murine primary cultured skeletal muscle cells with recombinant full-length human adiponectin, which was expressed in the mouse myeloma cell line NS0 and purified, and then we searched, using two-dimensional electrophoresis, for proteins upregulated more than threefold by adiponectin as compared with untreated cells. As confirmed by immunoblotting under nonreducing conditions (Fig. 1*E*), the adiponectin species used in this experiment may be atypical because these were essentially mixtures of the HMW and LMW isoforms of adiponectin, with little of the MMW form. The gels were stained with Coomassie brilliant blue (Fig. 1*A*) and scanned using a GS-800 calibrated densitometer, and gel images were analyzed. We selected 1,500 protein signals. Among these, only one protein was increased (6.3-fold) with adiponectin incubation. The protein spots in the

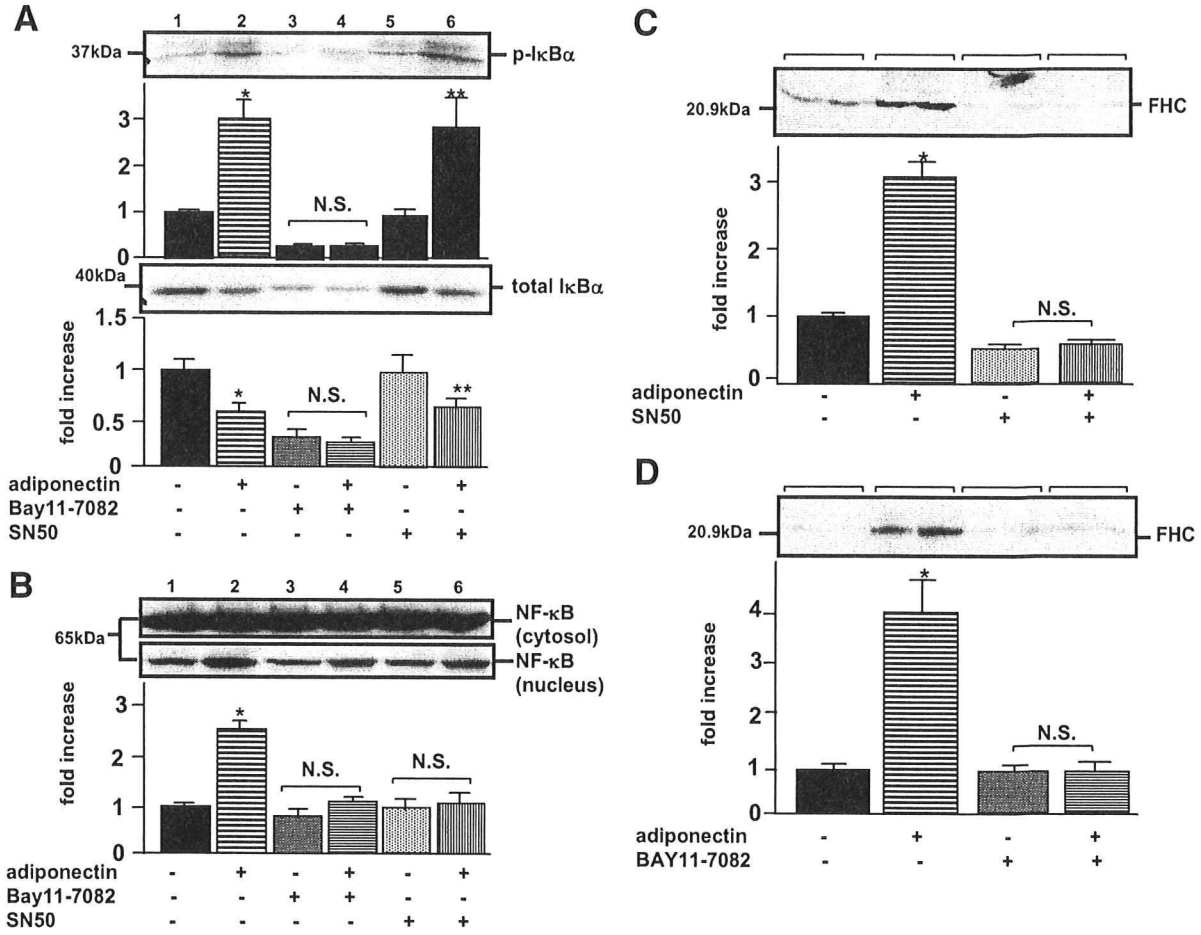

FIG. 2. Effects of IκB/NF-κB inhibitor on FHC in murine primary cultured skeletal muscle cells. Primary cultured skeletal muscle cells were pretreated with 100 μmol/l BAY11-7082 or 50 μg/ml NF-κB SN50 at 1 h before the cells were incubated with 40 μg/ml of adiponectin for 12 h. Cells were lysed in ice-cold lysis buffer and centrifuged at 14,000*g* for 10 min at 4°C. Supernatants including tissue protein extracts were subjected to SDS-PAGE. Transferred membranes were incubated for 1 h at room temperature with antibody against phosphor–IκB-α (*A*, *upper panel*), IκB-α (*A*, *lower panel*), p65 NF-κB (*B*), and FHC (*C* and *D*). After blotting with the indicated secondary antibody, detection was performed using an electrochemiluminescence chemiluminescent kit. Representative data (one sample each for *A* and *B*; two each for *C* and *D*) from four independent experiments (two samples for each experiment) are presented. Values are means ± SE. *Significant difference ($P < 0.05$) relative to IκB-α phosphorylation (*A*, *upper panel*), total IκB-α (*A*, *lower panel*), p65 NF-κB (*B*), or FHC expression (*C* and *D*) of control cells in the absence of adiponectin. **Significant difference ($P < 0.05$) relative to IκB-α phosphorylation (*A*, *upper panel*) or total IκB-α (*A*, *lower panel*) of paired control cells in the absence of adiponectin (*lane 5*). N.S., not significant relative to IκB-α phosphorylation (*A*, *upper panel*), total IκB-α (*A*, *lower panel*), p65 NF-κB (*B*), or FHC expression (*C* and *D*) of paired control cells in the absence of adiponectin.

absence or presence of adiponectin are indicated by the arrows in the magnified figure (Fig. 1*B*). We excised the protein spot from the gel (Fig. 1*B*, *right panel*) and identified four peptides, which were matched to FHC sequences (a.a.54–63, a.a.109–143, a.a.147–156, and a.a.158–172) using MALDI-TOF-MS analysis. The Score and Expect of the Mascot Search were 76 and 0.0022, respectively, both of which are highly definitive for FHC. As shown in Fig. 1*C*, FHC protein expressions were significantly increased in an adiponectin concentration–dependent manner but were unaffected by incubation with the same concentration of type I collagen or recombinant globular adiponectin, suggesting FHC upregulation to be specific to the multimer formation of adiponectin. Next, we assessed whether the expression of FLC is also upregulated by adiponectin. However, FLC expression was not altered (Fig. 1*D*).

NF-κB activation is involved in FHC upregulation by adiponectin. As FHC was reported to be transcriptionally upregulated in response to NF-κB activation (22), we next investigated whether adiponectin enhances NF-κB activity in primary skeletal muscle cells. The NF-κB bound to IκB-α is generally located in the cytosol before activation. In response to stimuli, IκB-α proteins are degraded, a process controlled by IκB-α phosphorylation, resulting in nuclear translocation of NF-κB and subsequent activation of NF-κB target gene transcription. When the cells were incubated with adiponectin, phosphorylation of IκB-α (Fig. 2*A*, *upper panel*, *lanes 1 and 2*) and a decrease in total IκB-α (Fig. 2*A*, *lower panel*, *lanes 1 and 2*) were observed, revealing that adiponectin actually stimulates NF-κB activation. The IκB-α phosphorylation required at least 3 h of incubation, suggesting that secondary effects might be involved in adiponectin-induced IκB-α phosphorylation. NF-κB SN50, an inhibitor of NF-κB translocation into the nucleus, did not affect the Iκ-B phosphorylation by adiponectin (Fig. 2*A*, *lanes 5 and 6*), whereas it was abolished by incubation with BAY11-7082, an inhibitor of IκB-α phosphorylation (Fig. 2*A*, *lanes 3 and 4*). To confirm that SN50 inhibits NF-κB translocation to the nucleus, we separated the myocyte-lysates into two compartments (i.e., nuclear extracts and cytosol) and performed immu-

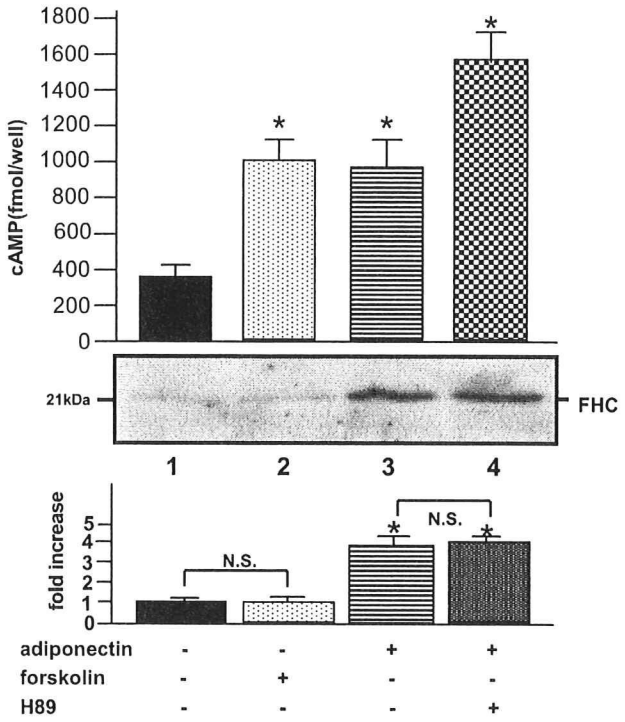

FIG. 3. Effects of recombinant human adiponectin on cAMP content of murine primary skeletal muscle cells. Primary skeletal muscle cells, cultured in 96-well plates, were exposed to 50 μg/ml of adiponectin and 5 μmol/l forskolin for 12 h. Adiponectin-treated cells were also pretreated with 1 μmol/l H89, a PKA inhibitor, for 1 h before the addition of adiponectin. The cAMP assay was performed according to the manufacturer's instructions. Cell lysates from primary cultured skeletal muscle cells were subjected to SDS-PAGE, followed by electrophoretic transfer to a nitrocellulose membrane. Membranes were incubated for 1 h at room temperature with antibody against mouse FHC. Detection was performed using an electrochemiluminescence chemiluminescent kit according to the manufacturer's instructions. Representative results from four independent experiments are presented. Values are means ± SE. *Significant difference ($P < 0.05$) relative to control cells in the absence of ligands (*lane 1*). N.S.; not significant relative to paired control cells in the absence of forskolin (*lane 1*) or H89 (*lane 3*).

noblotting using the anti-p65 NF-κB antibody. As shown in Fig. 2*B*, increases in nuclear NF-κB proteins were observed with adiponectin incubation (Fig. 2*B*, *lane 2*), indicating translocation of the activated NF-κB into the nucleus, whereas no significant translocation of NF-κB proteins was observed when both adiponectin and SN50 were present (Fig. 2*B*, *lane 6*). In addition, FHC upregulation by adiponectin was completely abolished by NF-κB SN50 (Fig. 2*C*) or BAY11-7082 (Fig. 2*D*), indicating that FHC was upregulated by adiponectin via an NF-κB–dependent pathway. Taking into consideration the reported upregulation of FHC by cAMP via a proximal *cis*-acting element containing the CCAAT motif (23), we further examined whether FHC is regulated by a cAMP–protein kinase A (PKA)-dependent pathway. When incubated with adiponectin, cAMP levels inside primary cultured muscle cells were increased by 2.8-fold with FHC upregulation (Fig. 3, *lane 2*). Unexpectedly, H89, a PKA inhibitor, failed to block this FHC upregulation by adiponectin (Fig. 3, *lane 4*). Furthermore, forskolin increased cAMP levels in these cells without FHC upregulation (Fig. 3, *lane 2*). These results suggest that cAMP elevation in response to adiponectin treatment was not associated with FHC upregulation.

The effects of adiponectin, TNF-α, and free fatty acids on NF-κB target gene in HUVECs. To investigate whether adiponectin increases FHC in other types of cultured cells, we further examined the NF-κB activation of HUVECs. When HUVECs were treated with adiponectin, ICAM-1, which is primarily regulated by the NF-κB transcription factor, was slightly, but significantly, increased (Fig. 4*A*). In contrast, TNF-α markedly increased ICAM-1 expression (Fig. 4*B*). These ICAM-1 inductions by adiponectin or TNF-α were both inhibited by the addition of BAY 11-7082. These results suggested that TNF-α upregulated ICAM-I via an NF-κB–dependent pathway in HUVECs to a far greater extent than adiponectin. In addition, we examined the synergistic effects of adiponectin and TNF-α on ICAM-1 expression. Unexpectedly, the induction of ICAM-1 by TNF-α was inhibited by further addition of adiponectin (Fig. 4*C*), indicating that TNF-α and adiponectin antagonized each other via the signaling pathways of these agents. This phenomenon, which was reported previously (7,24), was also observed in the actions of adiponectin and palmitate on ICAM-1 expression. Next, we examined the effects of these NF-κB activators on FHC expression in HUVECs. Although FHC expression was slightly increased by TNF-α, neither adiponectin nor palmitate treatment produced significant increases (Fig. 4*D*). Taken together, these observations indicated that induction of FHC by adiponectin does not occur in HUVECs despite the NF-κB activation, presumably due to the minor effect of adiponectin on NF-κB activation.

Recombinant FHC reduces ROS production induced by oxidative stress. To investigate the cytoprotective effects of FHC against forms of damage mediated by oxidative stresses or inflammatory cytokines, we transfected adenovirus expressing recombinant FHC into HUVECs and C2C12 myocytes. As the murine primary cells exhibited susceptibility to adenovirus infection, we performed this experiment with C2C12 myotubes. Before the ROS assay, we confirmed recombinant FHC to be overexpressed by immunoblotting using anti-murine FHC antibodies. With overexpression of recombinant FHC, 13 and 28% reductions in relative ROS accumulations were observed in HUVECs and C2C12 myotubes, respectively (Fig. 5). In addition, FHC had a major effect on reducing ROS accumulation induced by various forms of oxidative stress (i.e., 26% [Fe^{2+}], 18% [TNF-α], and 25% [high glucose] in HUVECs; and 26% [(Fe^{2+}], 20% [TNF-α], and 49% [4-hydroxynonenal] in C2C12 myotubes), indicating that FHC exerts cytoprotective effects by reducing the ROS accumulation induced by various oxidative stresses. When these cells were treated with adiponectin, ROS-reducing effects, which were similar to those obtained with FHC overexpression, were also observed (data not shown). Taken together, these findings indicated FHC upregulation by adiponectin in skeletal muscle cells to at least partially explain the ROS-reducing effects of adiponectin.

Increased expression of NF-κB target genes with adiponectin incubation and their contributions to the ROS-reducing effects of adiponectin. We further investigated NF-κB target gene expressions (e.g., MnSOD and iNOS) by quantitative PCR. As shown in Fig. 6, these proteins (FHC, MnSOD, and iNOS) were similarly upregulated by adiponectin incubation (3.6-, 1.6-, and 5.1-fold, respectively, in skeletal muscle cells and 4.3-, 1.8-, and 3.5-fold, respectively, in C2C12 myotubes). No MnSOD protein was identified on our two-dimensional electrophoresis search for proteins upregulated more than three-

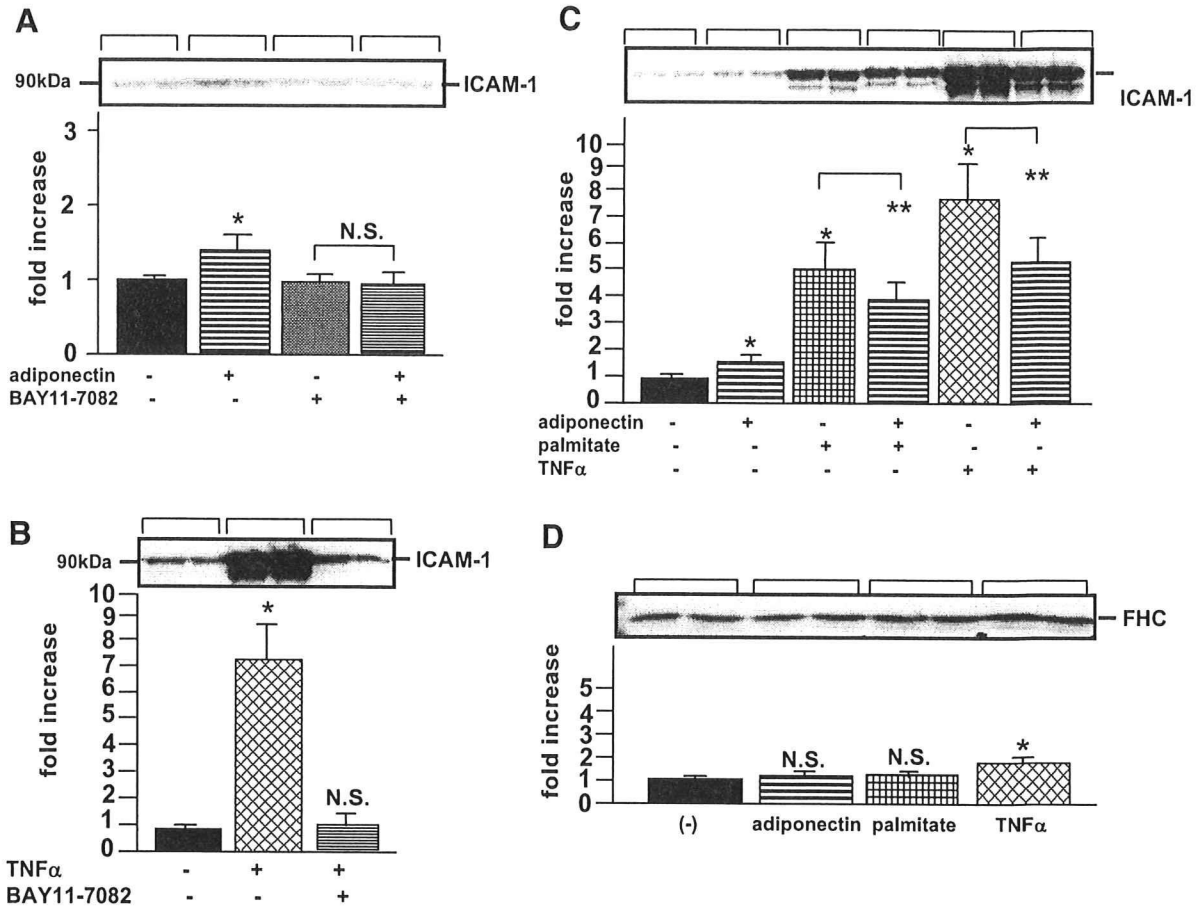

FIG. 4. Effects of recombinant human adiponectin, TNF-α, and free fatty acids on NF-κB–regulated gene expressions in HUVECs. After pretreating HUVECs with or without 100 μmol/l BAY11-7082 for 1 h, 25 μg/ml of adiponectin (*A*) or 10 ng/ml of TNF-α (*B*) were added, followed by incubation for 12 h. After HUVECs had been pretreated with or without 25 μg/ml of adiponectin for 1 h, 10 ng/ml of TNF-α or 0.4 mmol/l palmitate was added, followed by incubation for 12 h (*C* and *D*). Cell lysates from HUVECs were subjected to SDS-PAGE, followed by electrophoretic transfer to a nitrocellulose membrane. Membranes were incubated for 1 h at room temperature with antibody against ICAM-1 (*A*, *B*, and *C*) or FHC (*D*). Detection was performed using an electrochemiluminescence chemiluminescent kit according to the manufacturer's instructions. Representative data (each bracket) from four independent experiments (two samples for each experiment) are presented. Values are means ± SE. *Significant difference ($P < 0.05$) relative to ICAM-1 (*A–C*) and FHC (*D*) expressions in control cells in the absence of ligands. **Significant difference ($P < 0.05$) relative to ICAM-1 expression (*C*) in paired control cells in the absence of adiponectin but in the presence of palmitate (*lane 3*) or TNF-α (*lane 5*). N.S., not significant relative to FHC expression in control cells in the absence of adiponectin (*A*), TNF-α (*B*), and each ligand (*D*).

fold by adiponectin. Though the reason for our inability to identify iNOS in two-dimensional electrophoresis was not entirely clear, the minute amounts of iNOS proteins in skeletal muscles made this form of analysis impractical (25). To clarify the relevance of the observed increase in all three proteins to the changes in ROS, we investigated the ROS levels in C2C12 myotubes, in which the expressions of these three proteins were inhibited by induction of siRNAs. As shown in Fig. 7, under the condition in which no significant increases in the three gene products were observed with adiponectin incubation, we investigated adiponectin-induced changes in ROS accumulation. When FHC siRNAs were induced, we observed a marked decrease in the ROS-reducing effects of adiponectin incubation. On the other hand, there was no significant change in ROS accumulation with iNOS siRNA induction, while a slight but significant decrease was observed with MnSOD siRNA induction. These results suggest that increased FHC expression has a major impact on ROS accumulation; however, this increase does not explain the entire ROS-reducing effect of adiponectin.

Increased serum adiponectin upregulates FHC in skeletal muscles in vivo. To further confirm the FHC upregulation by adiponectin in in vivo experiments, we prepared mice expressing recombinant adiponectin by systemic adenovirus injection into the tail vein. Adenovirus gene transfer revealed ectopic overexpression of adiponectin in the liver to markedly upregulate serum adiponectin (control construct: 14.4 ± 0.6 μg/ml and adiponectin construct: 44.5 ± 4.9 μg/ml) (Fig. 8*B*). In particular, mainly the HMW and LMW forms of adiponectin were increased (Fig. 8*C*). As shown by immunoblotting of skeletal muscles, FHC expression in these muscles was increased 2.5-fold in adiponectin-transferred mice (Fig. 8*A*) (i.e., in vitro experiments confirmed FHC upregulation under physiological conditions).

DISCUSSION

Intensive previous studies (5,8) revealed adiponectin to improve insulin sensitivity and increase fatty acid oxidation in skeletal muscles. In fact, MMW or HMW adiponectin exerts these effects on skeletal muscles by activating

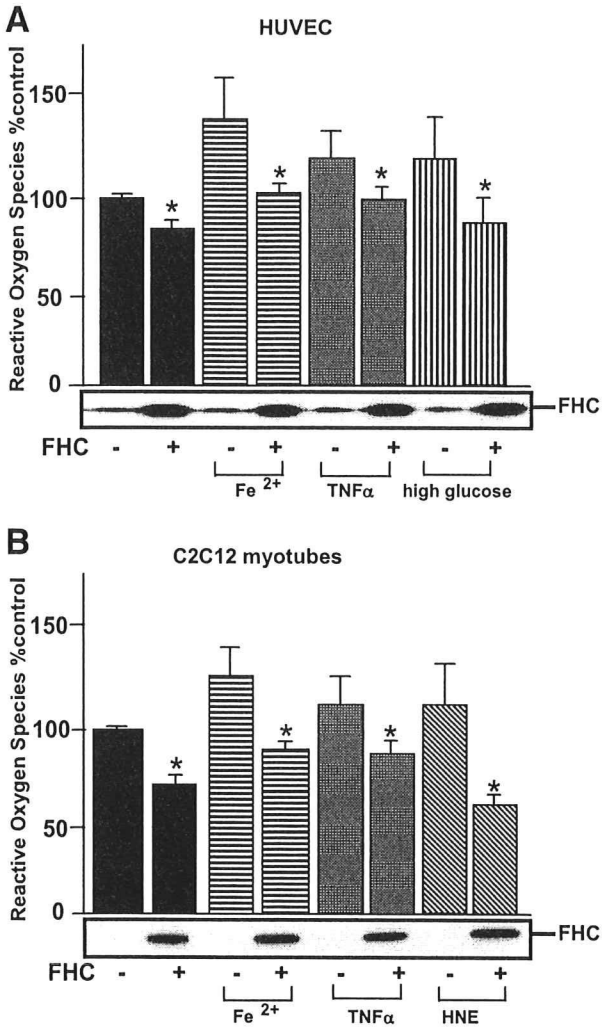

FIG. 5. Effects of recombinantly overexpressed FHC on ROS generation in C2C12 myotubes and HUVECs exposed to oxidative stresses. *A*: HUVECs, transfected with adenovirus overexpressing LacZ or recombinant FHC, were treated with 5.4 × 10^{-9} mol/l iron (II) sulfate heptahydrate and 25 mmol/l glucose. *B*: C2C12 myotubes, transfected with adenovirus overexpressing LacZ or recombinant FHC, were treated with 20 ng/ml of TNF-α and 100 μmol/l 4-hydroxynonenal (HNE). After a 24-h incubation, ROS generations were assayed by CM-H_2DCFDA oxidation-based fluorescence. Representative results from three independent experiments are presented. Values are means ± SE. *Significant difference (P < 0.05) relative to ROS production by paired control cells in the absence of FHC overexpression.

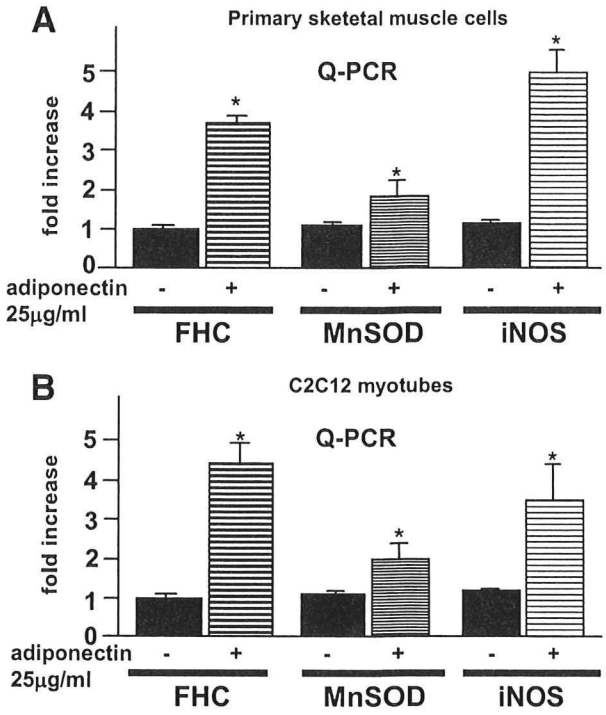

FIG. 6. FHC, MnSOD, and iNOS mRNA levels in primary skeletal muscle cells (*A*) and C2C12 myotubes (*B*) were determined by quantitative PCR using an ABI PRISM model 7000 according to the manufacturer's instructions. Each column shows the mean ± SE obtained from four samples in the presence or absence of adiponectin. *Significant difference (P < 0.05) relative to control cells in the absence of adiponectin.

AMP-activated protein kinase and peroxisome proliferator–activated receptor-α (26). On the other hand, HMW adiponectin was previously reported to activate NF-κB (10), the master coordinator of immunity, inflammation, differentiation, and cell survival (17,27–29). However, the physiological role of NF-κB activation in skeletal muscle cells has yet to be elucidated. In the present study, we treated murine primary cultured skeletal muscle cells with recombinant adiponectin and found FHC to be significantly increased. The two-dimensional gel electrophoresis–based proteomic approach used herein is generally acknowledged to be relatively insensitive in that it measures only a limited subset of tissue proteins and systematically excludes several classes. Adiponectin-induced FHC upregulation was seen only in cultured skeletal muscle cells, not endothelial cells (i.e., HUVECs). Judging from the small increase in ICAM-1 expression with adiponectin incubation, the NF-κB–activating effect of adiponectin was likely to be so small that we were unable to demonstrate FHC upregulation in HUVECs. These response differences between skeletal muscle and endothelial cells may be explained by variations in adiponectin species or different tissue localizations of molecules involved in adiponectin signaling, such as adiponectin receptors.

Our results demonstrate NF-κB activation to be involved in FHC upregulation by adiponectin. This mechanism of FHC upregulation is supported by the following data. First, in agreement with prior studies (10), we demonstrated that adiponectin does, in fact, really phosphorylate and degrade IκB-α in cultured skeletal muscle cells, thereby enhancing NF-κB activation. Second, FHC is regulated by NF-κB activation in response to enhanced oxidative stress (30). Third, FHC induction in response to adiponectin incubation is completely inhibited by BAY11-7082, an inhibitor of IκB-α phosphorylation, or NF-κB SN50, an inhibitor of NF-κB translocation into the nucleus. Though cAMP-dependent induction of FHC was previously demonstrated in human HeLa cells (31), our results show clearly that the cAMP/PKA pathway is not involved in FHC upregulation by adiponectin. Further study is needed to clarify the precise mechanisms by which FHC is regulated.

Ferritin is a major intracellular iron-storage protein that sequesters excess free iron molecules to minimize the generation of iron-catalyzed ROS (30,32). Ferritin consists of two subunits, FHC and FLC (15), and there are functional differences between these subunits. FHC has ferroxidase activity (i.e., the oxidation of Fe^{2+} to Fe^{3+}), which is involved in rapid iron uptake and release and is